View metadata, citation and similar papers at core.ac.uk

brought to you by CORE

provided by Queen's University Research Portal

Klebsiella pneumoniae survives within macrophages by avoiding delivery to lysosomes

Cano, V., March, C., Insua , J. L., Aguiló, N., Llobet, E., Moranta, D., ... Bengoechea, J. A. (2015). Klebsiella pneumoniae survives within macrophages by avoiding delivery to lysosomes. Cellular Microbiology, 17(11), 1537-1560. DOI: 10.1111/cmi.12466

Published in:
Cellular Microbiology

Document Version:
Peer reviewed version

Queen's University Belfast - Research Portal:
Link to publication record in Queen's University Belfast Research Portal

Publisher rights
©2015 John Wiley & Sons, Inc.
This is the peer reviewed version of the following article: Cano, V., March, C., Insua, J. L., Aguilo, N., Llobot, E., MorataD., Regueiro, V., Brenan, G. P., Millan-Lou, M. I., Martin, C., Garmendia, J., Bengoechea, J. A. (2015),Klebsiella pneumoniae survives within macrophages by avoiding delivery to lysosomes. Cellular Microbiology, VOL: PAGE NO's. which has been published in final form at http://onlinelibrary.wiley.com/doi/10.1111/cmi.12466/abstract. This article may be used for non-commercial purposes in accordance with Wiley Terms and Conditions for Self-Archiving.

General rights
Copyright for the publications made accessible via the Queen's University Belfast Research Portal is retained by the author(s) and / or other copyright owners and it is a condition of accessing these publications that users recognise and abide by the legal requirements associated with these rights.

Take down policy
The Research Portal is Queen's institutional repository that provides access to Queen's research output. Every effort has been made to ensure that content in the Research Portal does not infringe any person's rights, or applicable UK laws. If you discover content in the Research Portal that you believe breaches copyright or violates any law, please contact openaccess@qub.ac.uk.

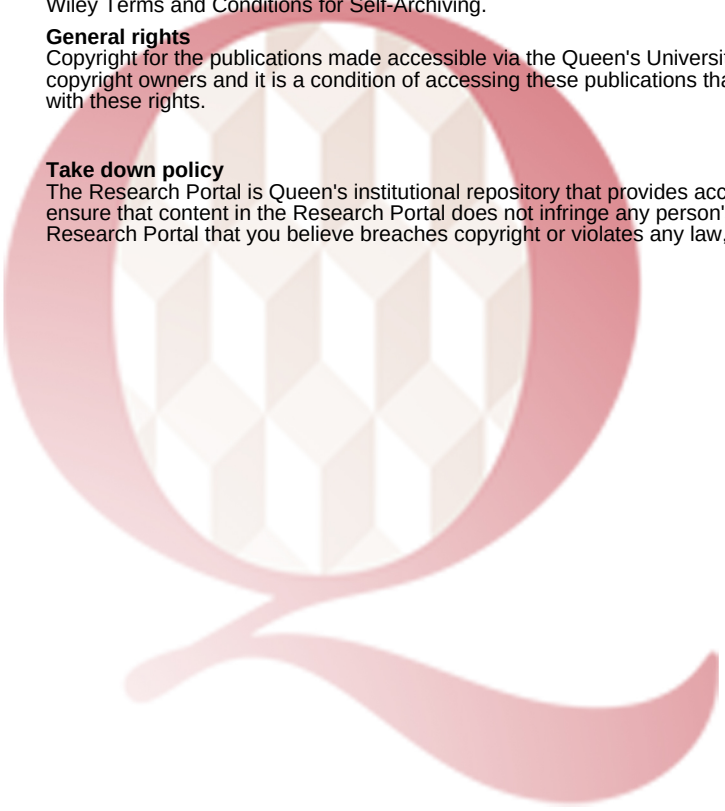

Download date:15. Feb. 2017

Klebsiella pneumoniae survives within macrophages by avoiding delivery to lysosomes.

Victoria Cano[1,2†],Catalina March[1,2†] , Jose Luis Insua[3†], Nacho Aguiló[2,5], Enrique Llobet[1,2,4], David Moranta[1,2,4], Verónica Regueiro[1,2,4], Gerry P Brenan[6], Maria Isabel Millán-Lou[2,5], Carlos Martín[2,5], Junkal Garmendia[2,7], José A. Bengoechea[3,8].

Laboratory Infection and Immunity, Fundació d'Investigació Sanitària de les Illes Balears (FISIB), Bunyola, Spain[1]; Centro de Investigación Biomédica en Red Enfermedades Respiratorias (CIBERES), Bunyola, Spain[2]; Centre for Infection and Immunity, Queen's University Belfast, Belfast, United Kingdom[3]; Institut d'Investigació Sanitària de Palma (IdISPa), Palma, Spain[4]; Grupo de Genética de Micobacterias, Dpto. Microbiología, Medicina Preventiva y Salud Pública, Universidad de Zaragoza, Zaragoza, Spain[5]; School of Biological Sciences, Queen's University Belfast, Belfast, United Kingdom[6]; Instituto de Agrobiotecnología, CSIC-Universidad Pública de Navarra-Gobierno de Navarra, Mutilva, Spain[7]; Consejo Superior de Investigaciones Científicas (CSIC), Madrid, Spain[8]

[†] These authors contributed equally to this work.

*Corresponding author:

Prof. José A. Bengoechea

Centre for Infection and Immunity,

Queen's University Belfast

Health Sciences Building,

97 Lisburn Rd. Belfast, UK BT9 7AE

Phone: +44 (0) 28 9097 2260; Fax: +44 (0) 28 9097 2671

E-mail: j.bengoechea@qub.ac.uk

Running title: *Klebsiella* intracellular survival

SUMMARY

Klebsiella pneumoniae **is an important cause of community-acquired and nosocomial pneumonia. Evidence indicates that *Klebsiell*a might be able to persist intracellularly within a vacuolar compartment. This study was designed to investigate the interaction between *Klebsiella* and macrophages. Engulfment of *K. pneumoniae* was dependent on host cytoskeleton, cell plasma membrane lipid rafts and the activation of PI 3-kinase (PI3K). Microscopy studies revealed that *K. pneumoniae* resides within a vacuolar compartment, the *Klebsiella* containing vacuolae (KCV), which traffics within vacuoles associated with the endocytic pathway. In contrast to UV-killed bacteria, the majority of live bacteria did not colocalize with markers of the lysosomal compartment. Our data suggest that *K. pneumoniae* triggers a programmed cell death in macrophages displaying features of apoptosis. Our efforts to identify the mechanism(s) whereby *K. pneumoniae* prevents the fusion of the lysosomes to the KCV uncovered the central role of the PI3K-Akt-Rab14 axis to control the phagosome maturation. Our data revealed that the capsule is dispensable for *Klebsiella* intracellular survival if bacteria were not opsonized. Furthermore, the environment found by *Klebsiella* within the KCV triggered the downregulation of the expression of *cps*. Altogether, this study proves evidence that *K. pneumoniae* survives killing by macrophages by manipulating phagosome maturation which may contribute to *Klebsiella* pathogenesis.**

INTRODUCTION

In the late nineteenth century, Eli Metchnikoff appreciated phagocytosis as a key process in the battle against pathogens. Phagocytosis can be conceptually divided into phagosome formation and its subsequent evolution into a degradative compartment, a process termed phagosome maturation. This is important because the nascent phagosome is not microbicidal. Maturation not only aids clearing infection, but also generates and routes antigens for presentation on MHC molecules in order to activate the adaptive immune system (Trombetta and Mellman. 2005). Phagosome maturation involves the sequential acquisition of different proteins, many of them of the endocytic pathway (Vieira *et al*. 2002,Flannagan *et al*. 2012). Thus, during and/or immediately after phagosome closure, the phagosome fuses with early endosomes, acquiring Rab5 and early endosome antigen 1 (EEA1). The phagosome rapidly loses the characteristics of early endosome and acquires late endosome features. The late phagosome is positive for Rab7, the mannose-6-phosphate receptor, lysobisphosphatidic acid, lysosome-associated membrane proteins (Lamps) and CD63. Ultimately, the organelle fuses with lysosomes to form the phagolysosome, identified by the presence of hydrolytic proteases, such as processed cathepsin D, cationic peptides and by an extremely acidic luminal pH which is regulated primarily by the vacuolar (V-type) ATP-ase complex. In the course of maturation, an oxidative system formed by the NADPH oxidase and ancillary proteins is also activated.

Many pathogens have developed strategies to counteract the microbicidal action of macrophages (Flannagan *et al*. 2009,Sarantis and Grinstein. 2012). Some pathogens inhibit phagocytosis. For example, the role of capsule polysaccharides in preventing opsonophagocytosis has been appreciated for many pathogens including *Neisseria meningitidis*, *Staphylococcus aureus* and *streptococci*. Others, such as enteropathogenic *Escherichia coli*, inhibit engulfment by blocking PI 3-kinase (PI3K) signaling whereas *Yersinia* species inhibits phagocytosis by injecting type III secretion effectors. Conversely, *Salmonella typhimurium* induces its own uptake and, once inside a modified phagosome, triggers macrophage death by a caspase-1 dependet process called pyroptosis

(Fink and Cookson. 2007). *Brucella* spp. resist an initial macrophage killing to replicate in a compartment segregated from the endocytic pathway with endoplasmic reticulum properties (von Bargen *et al*. 2012).

Klebsiella pneumoniae is a Gram negative capsulated pathogen which causes a wide range of infections, from urinary tract infections to pneumonia, being particularly devastating among immunocompromised patients with mortality rates between 25% and 60% (Sahly and Podschun. 1997). *K. pneumoniae* is an important cause of community-acquired pneumonia in individuals with impaired pulmonary defences and is a major pathogen for nosocomial pneumonia. Pulmonary infections are often characterized by a rapid clinical course thereby leaving very short time for an effective antibiotic treatment. *K. pneumoniae* isolates are frequently resistant to multiple antibiotics (Munoz-Price *et al*. 2013), which leads to a therapeutic dilemma. In turn, this stresses out the importance of pulmonary innate defense systems to clear *K. pneumoniae* infections.

Resident alveolar macrophages play a critical role in the clearance of bacteria from the lung by their capacity for phagocytosis and killing. It has been shown that depletion of alveolar macrophages results in reduced killing of *K. pneumoniae in vivo* (Broug-Holub *et al*. 1997,Cheung *et al*. 2000). This suggests that *Klebsiella* countermeasures against phagocytosis would be important virulence factors. Supporting this notion, *K. pneumoniae* capsule (CPS) reduces phagocytosis by neutrophils and macrophages (March *et al*. 2013,Cortes *et al*. 2002b,Regueiro *et al*. 2006,Alvarez *et al*. 2000) and CPS mutant strains are avirulent not being able to cause pneumonia and urinary tract infections (Cortes *et al*. 2002b,Lawlor *et al*. 2005,Camprubi *et al*. 1993).

K. pneumoniae has been largely considered as an extracellular pathogen. However, there are reports showing that *K. pneumoniae* is internalized *in vitro* by different cell types being able to persist intracellularly for at least 48 h (Oelschlaeger and Tall. 1997). It has been also reported the presence of intracellular *Klebsiella* spp. within a vacuolar compartment inside human macrophages, mouse alveolar macrophages and lung epithelial cells *in vivo* (Cortes *et al*. 2002b,Fevre *et al*. 2013,Willingham *et al*. 2009,Greco *et al*. 2012). The present study was designed to investigate the

interaction between *K. pneumoniae* and macrophages. We report that *K. pneumoniae* survives within macrophages by deviating from the canonical endocytic pathway and residing in a unique intracellular compartment which does not fuse with lysosomes. Mechanistically, our results indicate that *Klebsiella* targets the PI3K-Akt-Rab14 axis to control the phagosome maturation. Finally, we present evidence indicating that *K. pneumoniae* has the potential to kill and escape from the phagocyte.

RESULTS

K. pneumoniae survives inside macrophages.

To explore whether *K. pneumoniae* resides inside macrophages *in vivo*, macrophages were isolated from the bronchoalveolar lavage of mice infected intranasally with *K. pneumonia* strain 43816 (hereafter Kp43816R). Confocal microscopy experiments showed that 85 ± 4 % of the intracellular bacteria did not colocalize with the lysosomal marker cathepsin D (Fig 1A). Macrophages isolated obtained from the bronchoalveolar lavage were pulsed-chased with tetramethylrhodamine-labelled dextran (TR-dextran) as described in the Experimental procedures. Pulse-chase protocols with TR-dextran are extensively used in the literature to label lysosomes (Morey *et al*. 2011,Eissenberg *et al*. 1988,Hmama *et al*. 2004,Lamothe *et al*. 2007). Confocal microscopy revealed that 80 ± 3 % intracellular *Klebsiella* did not colocalize with TR-dextran (Fig 1A).

To assess the interaction of *K. pneumoniae* and macrophages in more detail, we standardized the infection conditions of the mouse macrophage cell line MH-S with Kp43816R. We optimized the time of bacteria-cell contact (30, 60 and 120 min), the multiplicity of infection (MOI) (100, 50 or 10 bacteria per cell), and the antibiotic treatment necessary to kill the remaining extracellular bacteria after the contact. To synchronize infection, plates were centrifuged at 200 x *g* during 5 min and intracellular bacteria were enumerated after macrophage lysis with 0.5% saponin in PBS. We found that 90 min treatment with a combination of gentamicin (300 μg/ml) and polymxyin B (15

μg/ml) was necessary to kill 99.9% of the extracellular bacteria. The highest numbers of engulfed bacteria were obtained after 120 min of bacteria-cell contact with a multiplicity of infection (MOI) of 100:1. However, these conditions also triggered a significant decrease in cell viability as detected by the trypan blue exclusion method. 30 min of contact and a MOI of 50:1 were the conditions in which no decrease in cell viability was observed and, therefore, they were used in the subsequent experiments described in this study.

To investigate the molecular mechanisms used by mouse macrophages to engulf Kp43816R, infections were carried out in the presence of inhibitors of host cell functions (Fig 1B). Cytochalasin D and nocodazol reduced the engulfment of Kp43816R hence indicating that Kp43816R phagocytosis requires the assembly of F-actin and the host microtubule network. Methyl-β-cyclodextrin (MβCD), which depletes cholesterol from host cell membranes, was employed to analyse the involvement of lipid rafts in Kp43816R phagocytosis. Cholesterol depletion impaired *Klebsiella* engulfment by MH-S. Similar results were obtained when cells were treated with filipin and nystatin (Fig. 1B). Since the generation of phosphoinositides is linked to phagosome formation (Vieira *et al*. 2001), we assessed the contribution of the PI3K signalling pathway on Kp43816R phagocytosis. Pre-treatment of MH-S cells with LY294002, a specific inhibitor of PI3K activity, resulted in the blockage of Kp43816R phagocytosis (Fig. 1B). Immunofluorescence experiments further confirmed that treatment of cells with LY294002 inhibited the engulfment of *Klebsiella* (Fig S1). This was also true for UV-killed bacteria (Fig S1). Akt is a downstream effector of PI3K which becomes phosphorylated upon activation of the PI3K signalling cascade. As expected, western blot analysis revealed that Kp43816R induces the phosphorylation of Akt in a PI3K-dependent manner since LY294002 inhibited *Klebsiella*-induced phosphorylation of Akt (Fig. 1C-D). UV-killed bacteria also induced the phosphorylation of Akt although the levels were significantly lower than those induced by live bacteria (Fig 1C). The PI3K-Akt cascade is also activated by Kp43816R in human macophages (THP-1 monocytes differentiated to macrophages by phorbol-12-myristate-13-acetate [PMA] treatment; hereafter mTHP-1) (Fig. S2).

Bacterial intracellular location in MH-S cells was assessed 3 and 6 h post infection by transmission electron microscopy (TEM). In good agreement with other published observations *in vivo* (Cortes *et al*. 2002b,Fevre *et al*. 2013,Willingham *et al*. 2009,Greco *et al*. 2012), bacteria were located in a vacuolar compartment (data not shown). To determine the fate of intracellular Kp43816R, MH-S cells were infected with GFP-expressing Kp43816R and the number of intracellular bacteria was assessed microscopically using differential (extracellular/intracellular) staining and by plating after different incubation times. The number of intracellular bacteria in MH-S cells decreased during the first 2 h of infection but then it remained constant until 7.5 h post infection (Fig 2A). Immunofluorescence analysis revealed that the number of infected macrophages decreased during the first 2 h hence suggesting that some cells are able to clear the infection. However, after 2 h, the percentage of infected macrophages did not change until the end of the experiment (Fig 2B). We did not observe any change of host cell morphology (data not shown). The majority of infected macrophages contained less than three bacteria (Fig 2C). The fact that the number of macrophages containing between three and five bacteria or more than five did not change over time suggests that there is not significant bacteria replication. Similar results were obtained when mTHP-1 cells were infected (Fig S3).

To elucidate whether those intracellular bacteria assessed by microscopy were indeed viable, cells were infected with *Klebsiella* harbouring two plasmids, one conferring constitutive expression of mCherry (pJT04mCherry) and another one (pMMB207gfp3.1) expressing *gfp* under the control of an IPTG inducible promoter. Therefore, only metabolically active bacteria will be mCherry-GFP positive. Microscopy analysis using differential (extracellular/intracellular) staining showed that more than 75% of intracellular bacteria were mCherry-GFP positive 3.5 h post infection (Fig 2D-E). This percentage did not change over time. To further confirm that intracellular *Klebsiella* are metabolically active, fluorescent *in situ* hybridisation (FISH) was carried out by using the oligonucleotide probes EUB338 and GAM42a (see Experimental procedures). The detection of bacteria by these oligonucleotide probes is dependent on the presence of sufficient ribosomes per

cell, hence providing qualitative information on the physiological state of the bacteria (Christensen *et al*. 1999,Morey *et al*. 2011). Microscopy analysis revealed that the number of bacteria metabolically active (FISH positive) *versus* the total number of intracellular bacteria (GFP positive) was maintained through the infection (Fig. S4).

Collectively, these results showed that Kp43816R phagocytosis by macrophages is an event dependent on host cytoskeleton and cell plasma membrane lipid rafts. Moreover, the PI3K/Akt host signalling pathway is activated by Kp43816R infection and it is required for bacterial phagocytosis. Our data demonstrate that Kp43816R survives within macrophages through the course of infection and the TEM experiments may suggest that Kp43816R may reside in a specific compartment that we named the *Klebsiella* containing vacuole (KCV).

K. pneumoniae elicits a cytotoxic effect on macrophages.

Examination of the infected monolayers by immunofluorescence at different time points revealed a decreased in the overall monolayer density at 10 h post infection which became more evident 20 h post infection (Fig S5A). This observation prompted us to study whether Kp43816R exerts a cytotoxic effect on macrophages. We assessed the viability of infected MH-S cells by measuring the levels of LDH release. Kp43816R infection was associated with a 35% decrease in cell viability after 20 h of infection. Kp43816R-triggered cytotoxic effect on macrophages was also evident when cell viability was estimated by the neutral red uptake assay (Fig S5B).

The induction of host cell apoptosis is one mechanism used by some pathogens to augment infection (Navarre and Zychlinsky. 2000). To test whether Kp43816R causes apoptosis of MH-S cells, apoptosis was measured with annexin V, to analyze phosphatidylserine translocation to the outer leaflet of the plasma membrane, and 7-actinomycin D (AAD) to evaluate plasma membrane integrity. Flow cytometry analysis of infected cells showed a significant increased in annexin V^+AAD^- cells over time (Fig. 3). The amount of double-positive annexinV^+AAD^+ cells, which corresponds to a necrotic-like phenotype, was markedly lower than the amount of cells annexin

V^+AAD^- at all times analyzed. These results indicate phosphatidylserine translocation and intact membrane integrity, a classical apoptotic phenotype, hence suggesting that Kp43816R triggers apoptosis in macrophages.

K. pneumoniae prevents phagosome fusion with lysosomes.

Because Kp43816R is able to survive within macrophages, we hypothesized that *Klebsiella* must either divert the normal process of phagosome maturation or withstand the hostile environment of the mature phagolysosome. Therefore, we analyzed the maturation of the KCV during the course of an infection by unravelling the association of the KCV with compartments of the exocytic and endocytic pathways. Bacteria did not colocalize with either markers of the endoplasmic reticulum (calnexin) or markers of the Golgi network (GM 130) at any time point analyzed (Fig S6). EEA1 is an early endosome-specific peripheral membrane protein which colocalizes with the small GTP binding protein Rab5 (Vieira *et al*. 2002,Flannagan *et al*. 2012). As shown in Figure 4, we could detect the presence of EEA1 on 22 ± 4% of KCVs at 15 min post infection. The percentage of vacuoles positive for this marker dropped to 15 ± 9% and to 5 ± 1% at 60 and 90 min post infection, respectively (Fig 4). We next sought to determine whether the KCV acquires the late endosomal markers Lamp1 and Rab7 (Vieira *et al*. 2002,Flannagan *et al*. 2012). KCVs were positive for Lamp1 already at 15 min post infection and the percentage of positive KCVs increased over time (Fig 4). KCVs remained positive for Lamp1 until 7.5 h post infection. Rab7 is a small GTPase that controls vesicular transport to late endosomes and lysosomes in the endocytic pathway (Rink *et al*. 2005). To assess the presence of Rab7 on KCVs, macrophages were transfected with GFP-Rab7 and then infected with Kp43816R. The majority of the vacuoles containing Kp43816R were positive for both Rab7 and Lamp1 (Fig 4). To determine the activation status of Rab7 we asked whether RILP, a Rab7 effector protein that exclusively recognizes the active (GTP bound) conformation of Rab7 (Cantalupo *et al*. 2001,Jordens *et al*. 2001), labels the KCV. Before infection, cells were transfected with a plasmid containing GFP fused to the C-

terminal Rab7-binding domain of RILP, called “RILP-C33”, which can be used as a reliable index of the presence and distribution of active Rab7 (Cantalupo *et al*. 2001,Jordens *et al*. 2001). As shown in Figure 4 RILP-C33-EGFP colocalized with the majority of KCVs. These vacuoles were also positive for Lamp1.

Since the interaction of Rab7 with RILP drives fusion with lysosomes (Cantalupo *et al*. 2001,Jordens *et al*. 2001), we sought to determine whether KCV colocalizes with lysosomal markers. Although there are not markers that unambiguously distinguish late endosomes from lysosomes, mounting evidence indicates that an acidic luminal pH and the presence of hydrolytic proteases, such as processed cathepsin D, are characteristics of the phagolysosomal fusion (Vieira *et al*. 2002,Flannagan *et al*. 2012). We used the fixable acidotropic probe LysoTracker to monitor acidic organelles in infected macrophages. We found a major overlap between the dye and the KCVs (Fig 5), hence indicating that the KCV is acidic. We next examined the presence in the vacuole of cathepsin D as a marker for the lysosomal soluble content. The majority of the KCVs did not colocalize with cathepsin D (Fig 5), thereby suggesting that the KCV does not fuse with lysosomes. To further sustain this notion, we assessed KCV colocalization with TR-dextran. Prior to bacterial infection macrophages were pulsed with TR-dextran for 2 h followed by a 1 h chase in dye-free medium to ensure that the probe is delivered from early and recycling endosomes to phagolysosomes (Morey *et al*. 2011,Eissenberg *et al*. 1988,Hmama *et al*. 2004,Lamothe *et al*. 2007). Confocal immunofluorescence showed that the majority of the KCVs did not colocalize with TR-dextran (Fig 5B). In contrast, when macrophages were infected with UV-killed Kp43816R more than 70% of the KCVs did colocalize with cathepsin D and TR-dextran 1.5 h post infection (Fig S7). Collectively, these results strongly support the notion that the majority of KCVs containing live bacteria prevent the fusion of the vacuole with lysosomes.

Similar findings were obtained when mTHP-1 cells were infected. KCV was not associated with compartments of the exocytic pathway, either Golgi network or endoplasmic reticulum, but acquired markers of the endocytic pathway, EEA1 and Lamp1 (Fig S8A). The majority of KCVs

colocalized with LysoTracker (Fig S8A) but they were negative for cathepsin D (Fig S8B). In contrast, nearly 70% of UV-killed Kp43816R colocalized with cathepsin D after 2 h post infection (Fig S8B). Altogether, these results indicate that only phagosomes containing UV-killed *Klebsiella* bacteria fuse with lysosomes in human macrophages.

In summary, these findings suggest that *K. pneumoniae* trafficks inside macrophages within vacuoles associated to the endocytic pathway, and that live bacteria perturb the fusion of the KCV with the hydrolases-rich lysosomal compartment.

Inhibition of compartment acidification affects *K. pneumoniae* intracellular survival.

Phagosome acidification has been shown to be essential for the intracellular survival of several pathogens (Morey *et al*. 2011,Ghigo *et al*. 2002,Porte *et al*. 1999). Therefore, we investigated the effect of inhibiting KCV acidification on *K. pneumoniae* survival. Bafilomycin A_1 is a specific inhibitor of the vacuolar type H+-ATPase in cells, and inhibits the acidification of organelles containing this enzyme, such as lysosomes and endosomes. As expected, phagolysosomal acidification was sensitive to bafilomycin A_1 treatment (Fig 6A), hence confirming dependence on the vacuolar H^+-ATPase. Moreover, bafilomycin A_1 treatment also abrogated the overlap between Kp43816R and the probe LysoTracker (Fig 6A). To assess the effect of vacuolar acidification on Kp43816R survival, cells were treated with bafilomycin A_1 at the onset of the gentamicin treatment and bacteria were enumerated by plating at different time points. Data shown in Figure 6C revealed that the number of intracellular Kp43816R decreased in bafilomycin A_1 treated cells over time compared to infected untreated cells. Control experiments revealed that bafilomycin A_1 has no toxic effect on *K. pneumoniae* (our control experiments [data not shown]) or on other Gram-negative bacteria (Morey *et al*. 2011,Porte *et al*. 1999)). Microscopy analysis revealed that the percentages of Kp43186R colocalization with TR-dextran in bafilomycin A_1 treated cells either at 3.5 or 5.5 h post infection (19± 4 and 20 ± 5%, respectively) were similar to those in DMSO (vehicle solution)-treated cells (20 ± 4 and 24 ± 6 %, respectively). In turn, the

percentage of mCherry-GFP positive intracellular bacteria dropped from 85 ± 7 % in DMSO-treated cells to 25 ± 4 % in bafilomycin A_1 treated cells already at 2.5 h post infection ($P < 0.05$ Mann-Whitney U test). Altogether, these observations suggest that Kp43816R intracellular survival requires KCV acidification.

PI3K-AKT and Rab14 contribute to *K. pneumoniae* intracellular survival.

S. enterica serovar *typhimurium* perturbs the fusion of the phagosomes with lysosomes by activating the host kinase Akt (Kuijl *et al*. 2007). In turn, inhibition of Akt activation reduces *Salmonella* intracellular survival (Kuijl *et al*. 2007,Chiu *et al*. 2009). Several pathogens also target the PI3K-Akt axis to manipulate cell biology for their own benefit (Krachler *et al*. 2011). Since Kp43816R induced the activation of Akt in a PI3K-dependent manner we sought to determine the contribution of the PI3K-Akt axis to the intracellular survival of *K. pneumoniae*. Treatment of cells with the PI3K inhibitor LY294002 or the Akt inhibitor AKT X at the onset of the gentamicin treatment reduced the number of intracellular bacteria in MH-S cells (Fig 7A). Moreover, microscopy analysis revealed that more than 70% bacteria colocalized with either TR-dextran or cathepsin D in cells treated with AKT X (Fig 7B and Fig S9). Collectively, these results support the notion that Kp43816R targets the PI3K-Akt axis to survive intracellularly.

At least 18 Rab GTPases are implicated in phagosomal maturation (Smith *et al*. 2007). Interestingly, *Salmonella* targets Rab14 to prevent phagosomal maturation in an Akt dependent manner (Kuijl *et al*. 2007). We speculated that Kp43816R may also target Rab14 to control the maturation of the phagosome. Immunofluorescence experiments revealed that GFP-Rab14 colocalized with the KCVs (Fig 7C-D). To determine whether Rab14recruitment is required for intracellular survival, cells were transfected with a Rab14 dominant-negative construct (DN-Rab14) or control vector and then infected with Kp43816R. As shown in figure 7E, we found a 60% decrease in the number of intracellular bacteria in cells transfected with DN-Rab14. Supporting that *Klebsiella* recruited Rab14 to the KVC in an Akt-dependent manner, GFP-Rab14 did not colocalize

with the KCV in AKT X treated cells (7 ± 2 % percentage of colocalization at 2.5 h post infection) (Fig 7F).

In summary, our results are consistent with a model where Kp43816R targets the PI3K-Akt-Rab14 axis to control the phagosome maturation to survive inside macrophages.

K. pneumoniae capsule polysaccharide is dispensable for intracellular survival.

We were keen to identify *K. pneumoniae* factors necessary for intracellular survival. Given the importance of *K. pneumoniae* CPS on host-pathogen interactions, we explored whether CPS is also necessary for *K. pneumoniae* intracellular survival. As anticipated, a CPS mutant was engulfed by MH-S and mTHP1 macrophages in higher numbers than Kp43816R (data not shown). For the sake of comparison with the wild-type strain in time-course experiments, we adjusted the MOI of the CPS mutant to get comparable numbers of intracellular bacteria at the beginning of the infection. Time course experiments showed no differences between the number of intracellular bacteria of both strains in MH-S and mTHP1 cells (Fig 8A).

Given the critical role of CPS in preventing complement-mediated opsonophagocytosis (Alvarez *et al*. 2000,de Astorza *et al*. 2004,Cortes *et al*. 2002a), we evaluated whether the intracellular fate of the CPS mutant could be modified by bacterial opsonization with human serum. In agreement with previous reports (de Astorza *et al*. 2004,Cortes *et al*. 2002a), opsonization of the CPS mutant resulted in an increase in the number of ingested bacteria by mTHP1 cells compared to nonopsonized bacteria (Fig 8B). Fort he sake of comparison, the MOI was adjusted to get comparable numbers of intracellular bacteria at the beginning of the infection. The number of CFU recovered from cells infected with the opsonized CPS mutant was significantly lower than the number of CFU recovered from cells infected with non-opsonized bacteria (100 fold lower at 8 h post infection; Fig 8C). These data indicate that internalization via the C3 receptor results in a significant loss of intracellular viability, presumably because these bacteria are ultimately delivered to lysosomes.

The lack of contribution of CPS to intracellular survival prompted us to analyze the expression of *cps* in the KCV. To monitor *cps* expression over time, we generated a transcriptional fusion in which the *cps* promoter region was cloned upstream a promoterless *gfp* that encodes a protein tagged at the C terminus with the (LVA) peptide. The GFP(LVA) protein is targeted for Tsp protease degradation within the bacteria and has been reported to have 40-min half-life, while untagged GFP is very stable (estimated *in vivo* half-life, 24 h) (Miller *et al*. 2000). We assessed GFP fluorescence in Kp43816R containing the unstable GFP reporter grown in LB. *Klebsiella* was stained using rabbit anti-*Klebsiella* serum followed by Rhodamine-conjugated donkey anti-rabbit secondary antibody. FACS analysis revealed an overlap between GFP fluorescence (green histogram) and Rhodamine fluorescence (red histogram) in bacteria grown in LB (Fig 8D, panel label as inoculum) which is in perfect agreement with the constitutive expression of *cps* by bacteria grown in LB. To investigate *cps* expression in intracellular bacteria, MH-S cells were infected with Kp43816R containing the GFP reporter. Cells were processed as described in Experimental procedures, and fluorescence analysed by FACS at different time points post infection. GFP fluorescence (green histograms) was measured in the gated Rhodamine positive population (red histograms). Data in Figure 8D shows that GFP fluorescence decreased over time in the intracellular bacteria reaching the levels of the control strain carrying the empty vector (grey histogram), which is considered negative for GFP fluorescence.

To explore whether the acidic pH of the KCV might be responsible for the downregulation of *cps* expression, bacteria were grown in M9 mininal medium, with 8 μM magnesium sulfate, buffered to different pHs. The expression of the *cps::gfp* fusion was 5-fold lower when bacteria were grown at pH 5.5 than at pH 7.5 (Fig 8E). Similar results were obtained when the mRNA levels of *wzi*, *orf7* and *gnd*, three genes of the *cps* operon (Arakawa *et al*. 1995), were assessed by real time quantitative PCR (RT-qPCR) (Fig 8F).

Collectively, these findings show that *K. pneumoniae* CPS is dispensable for intracellular survival. In fact, the environment found by *Klebsiella* within the KCV triggers the downregulation

of the expression of *cps*. The fact that opsonization affects the intracellular survival of the CPS mutant indicates that the mechanism of bacteria entry into macrophages has a major impact in the ability of *K. pneumoniae* to survive intracellularly.

DISCUSSION

In this work, we present compelling evidence demonstrating that *K. pneumoniae* survives killing by macrophages by manipulating phagosome maturation. Our data sustain that *K. pneumoniae* traffics within vacuoles associated with the endocytic pathway in mouse and human macrophages. In contrast to UV-killed bacteria, which colocalize with lysosomal markers, live bacteria modify the vacuole biogenesis preventing the fusion of the KCV with the hydrolases-rich lysosomal compartment. *K. pneumoniae* thus increases the list of pathogens able to alter phagosome maturation.

Engulfment of *K. pneumoniae* by mouse and human macrophages was dependent on host cytoskeleton, cell plasma membrane lipid rafts and the activation of PI3K which are all commonly needed to engulf pathogens and inert particles such as latex beads (Vieira *et al*. 2002,Flannagan *et al*. 2012). TEM analysis suggested that *K. pneumoniae* resides inside a vacuolar compartment and, by using FISH and two fluorescent markers tagging, we confirmed that intracellular bacteria are metabolically active. Several lines of evidence indicate that *K. pneumoniae* infections are associated with cell death (Willingham *et al*. 2009,Cano *et al*. 2009,Cai *et al*. 2012). In good agreement, in this study we show that *K. pneumoniae* triggers a programmed cell death in macrophages displaying features of apoptosis. Of note, kinase activity profiling in whole lungs during *K. pneumoniae* infection showed the activation of kinases associated to induction of apoptosis (Hoogendijk *et al*. 2011). However, Willingham and co-workers reported that *K. pneumoniae* activates the NLRP3-dependent cell death programme termed pyronecrosis (Willingham *et al*. 2009). Similar apparently contradictory findings have been reported for *Shigella flexneri* infections. *Shigella* triggers apoptotic and pyroptotic cell death in macrophages depending on the bacterial dosage and time of

385 infection (Willingham *et al*. 2007,Hilbi *et al*. 1998). In that case, short time of bacteria-cell contact
386 and low MOI are associated to induction of apoptosis (Willingham *et al*. 2007,Hilbi *et al*. 1998).
387 Notably, the infection conditions in our study are different to those used by Willingham and co-
388 workers who used a MOI four times higher than ours (Willingham *et al*. 2009). Future studies are
389 warranted to carefully assess the influence of infection conditions on *Klebsiella*-induced cell death.

390 Manipulation of cell death is a common pathogenic strategy not only for bacteria but also for
391 viruses (Finlay and McFadden. 2006). In general, viruses either accelerate or inhibit apoptosis of
392 the infected cell, depending on the biology of the specific virus. Like viruses, obligate intracellular
393 bacteria generally suppress apoptotic death. Because apoptosis is a less inflammatory process than
394 necrotic death, many nonobligate intracellular pathogens trigger apoptotic death to avoid cell to cell
395 communications. Thus, *Klebsiella*-induced macrophage death by apoptosis could be considered a
396 central aspect of *Klebsiella* infection biology taken into account the evidence demonstrating that
397 alveolar macrophages play a critical role in the clearance of *Klebsiella* (Broug-Holub *et al*.
398 1997,Cheung *et al*. 2000) and the importance of an early inflammatory responses to control the
399 infection (Greenberger *et al*. 1996a,Greenberger *et al*. 1996b,Happel *et al*. 2005,Happel *et al*.
400 2003).

401 The vacuole of *K. pneumoniae* and its biogenesis was studied by immunofluorescence. The
402 presence of EEA1 on the KCV indicates that internalized bacteria are initially present in a vacuole
403 related to the endocytic pathway. However, *K. pneumoniae* does not remain in early endosomes as
404 demonstrated by the acquisition of Lamp1 and Rab7. A hallmark of the maturation is the exclusion
405 of lysosomal hydrolases in the majority of KCVs containing live bacteria. In contrast, more than
406 50% of the KCVs containing UV-killed bacteria were positive for lysosomal markers already 90
407 min post infection. The KCV is acidic most likely due to the activity of vacuolar proton-ATPases.
408 Notably, inhibition of these pumps by bafilomycin A_1 resulted in a decrease in intracellular
409 bacterial numbers. Similar findings have been reported for non typable *H. influenza*e, *Tropheryma*
410 *whipplei*, and *Brucella suis* (Morey *et al*. 2011,Ghigo *et al*. 2002,Porte *et al*. 1999). The reduction

411 of intracellular viability may have several explanations. Bafilomycin A_1 might affect other
412 macrophage functions necessary for *K. pneumoniae* survival. An alternative hypothesis, and more
413 appealing to us, is that *K. pneumoniae* requires a low pH environment for survival within the KCV
414 which is in agreement with our data showing a significant decrease in the number of metabolic
415 active intracellular bacteria in bafilomycin A_1-treated cells. For example, the acidic environment
416 may facilitate the uptake of nutrients by *Klebsiella*. Acidic pH is required for the transport of
417 glucose in *Coxiella burnetii* (Howe and Mallavia. 2000) and localization in an acidic environment
418 facilitates the availability of iron for the growth of *Francisella turalensis* (Fortier *et al*. 1995). In
419 addition, low pH may regulate the expression of factors essential for intracellular survival. This has
420 been shown to be true for virulence gene transcription in *S. typhimurium* (Yu *et al*. 2010). In this
421 context, our data revealed that *Klebsiella* downregulates the expression of *cps* when residing within
422 the KCV. Interestingly, when *Klebsiella* was cultured in low magnesium and acidic pH we also
423 found a downregulation of *cps* expression. It is tempting to speculate that these signals could trigger
424 *cps* downregulation within the KCV. In fact, we show here that the KCV is acidic and there are
425 reports suggesting that the magnesium concentration in pathogen-containing vacuoles is in the
426 micromolar range (Garcia-del Portillo *et al*. 1992). Future efforts will be devoted to characterize the
427 chemical composition of the KCV as well as the transcriptional landscape of intracellular *K.*
428 *pneumoniae*.

429 It was interesting to consider the mechanism(s) whereby *K. pneumoniae* prevents the fusion
430 of the lysosomes to the KCV. The overall resemblance between the KCV and the *Salmonella*
431 containing vacuole (acidic Lamp-1-positive cathepsin-negative vacuole) prompted us to explore
432 whether *K. pneumoniae* employs similar strategies as *Salmonella* to subvert phagosome maturation.
433 Kuijl and coworkers (Kuijl *et al*. 2007) demonstrated that *S. typhimurium* activates Akt to prevent
434 phagosome-lysosome fusion. Since *K. pneumoniae* activates Akt *in vitro* (this work and (Frank *et*
435 *al*. 2013)) and *in vivo* (Hoogendijk *et al*. 2011) we speculated that activated Akt may also promote
436 *Klebsiella* intracellular survival. Indeed this was the case. Akt inhibition resulted in a significant

decrease in bacterial intracellular survival associated with an increased colocalization of the KCV with lysosomal markers. The fact that Akt is implicated in the intracellular survival of other pathogens, including *M. tuberculosis* (Kuijl *et al*. 2007), strongly suggests that this kinase is a central host node targeted by pathogens to take control over cellular functions.

PI3K/Akt governs phagosome maturation by controlling, at least, the activation of Rab GTPases (Thi and Reiner. 2012), although Rab14 is emerging as a central Rab in this process. Previous data indicate that pathogens hijack Rab14 to manipulate phagosome maturation. The *M. tuberculosis* vacuole recruits and retains Rab14 to maintain early endosomal characteristics (Kyei *et al*. 2006) whereas *S. typhimurium* containing vacuole retains Rab14 in an Akt-dependent manner to arrest phagosome maturation (Kuijl *et al*. 2007). Immunofluorescence confirmed that the KCV is positive for Rab14 in an Akt-dependent manner whereas transient transfection of the dominant-negative Rab14 resulted in a decrease in bacteria intracellular survival. In aggregate, this evidence supports a scenario in which *K. pneumoniae* manipulates phagosome maturation by targeting a PI3K-Akt-Rab14 pathway. Nevertheless, we do not rule out that there are additional pathways necesary for *Klebsiella* intracellular survival.

We were keen to identify the bacterial factors interfering with the phagosomal maturation pathway. Given the critical role of *K. pneumoniae* CPS in preventing host defense responses (March *et al*. 2013,Regueiro *et al*. 2006,Lawlor *et al*. 2005,Frank *et al*. 2013,Moranta *et al*. 2010,Campos *et al*. 2004,Lawlor *et al*. 2006), we hypothesized that CPS is necessary for intracellular survival. To our initial surprise, CPS does not play a large role, if any, in intracellular survival of *Klebsiella* since a *cps* mutant did not display any loss of viability upon phagocytosis. Furthermore, the *cps* mutant also triggered a programmed cell death in macrophages (data not shown). At first glance, these findings may seem contradictory with the well-established role of CPS in *K. pneumoniae* virulence. However, considering the presence of complement in the bronchoalveolar fluid (Wu *et al*. 2005), the fact that opsonization results in more efficient internalization of pathogens and maturation of phagosomes (Aderem and Underhill. 1999), and the well-known role of CPS in

preventing complement opsonization (de Astorza *et al*. 2004,Cortes *et al*. 2002a), we hypothesized that the *cps* mutant opsonization is deleterious to its intracellular fate. Indeed, this was the case hence revealing the critical role of CPS on *Klebsiella*-macrophage interplay. These results also illustrate how the mode of entry of a pathogen influences its intracellular outcome. Similar findings have been reported for other pathogens (Geier and Celli. 2011,Gordon *et al*. 2000,Drevets *et al*. 1993) but it cannot be considered a general feature since complement opsonization does not affect the intracellular fate of *Salmonella* and *M. tuberculosis* (Drecktrah *et al*. 2006,Zimmerli *et al*. 1996).

At present we can only speculate why *Klebsiella* downregulates the expression of *cps* once inside the KCV. Since CPS biosynthesis is a metabolically demanding process, *Klebsiella* may downregulate *cps* expression to better survive in the intracellular environment poor in nutrients. It is also plausible that CPS may interfiere with *Klebsiella* factors implicated in the intracellular survival. Current efforts of the laboratory are devoted to identify these factors.

Finally, it is worthwhile commenting on the clinical implications of this study. The antibiotics commonly used to treat *Klebsiella* infections are not very efficient against intracellular bacteria. In turn, our findings provide rationale for the use of inhibitors targeting the PI3K-Akt signaling cascade to eliminate intracellular *K. pneumoniae*. The concept of eradicating pathogens through targeting host factors modulated by pathogens has received wide attention in the infectious disease arena. Several promising drugs have been developed or are being developed to antagonize PI3K/Akt due to its relevance for many human cancers. Of note, there are *in vitro* and *in vivo* studies supporting the use of Akt inhibitors to eliminate intracellular *Salmonella* and *M. tuberculosis* (Kuijl *et al*. 2007,Chiu *et al*. 2009). Therefore, we propose that agents targeting PI3K/Akt might provide selective alternatives to manage *K. pneumoniae* pneumonias. Careful designed preclinical trials using the well establish mouse pneumonia model are warranted to test this hypothesis.

EXPERIMENTAL PROCEDURES

Bacterial strains and growth conditions.

Kp43816R is a rifampicin-resistant derivative of *K. pneumoniae* pneumonia clinical isolate [ATCC 43816; (Bakker-Woudenberg *et al.* 1985)]. This strain has been widely used to study the host response to Gram-negative pneumonia because it recapitulates acute pneumonia with fatal systemic spread at a relatively low infectious dose. Kp43816R expresses a type 1 O-polysaccharide and a type 2 capsule. Bacteria were grown in lysogeny broth (LB) at 37ºC on an orbital shaker (180 rpm). To UV kill bacteria, samples were UV irradiated (1 joule for 15 min) in a BIO-LINK BLX crosslinker (Vilber Lourmat). When appropriate, antibiotics were added to the growth medium at the following concentrations: rifampicin (Rif) 50 µg/ml, ampicillin (Amp), 100 µg/ml for *K. pneumoniae* and 50 µg/ml for *E. coli*; kanamycin (Km) 100 µg/ml; chloramphenicol (Cm) 12.5 µg/ml.

Construction of a *K. pneumoniae cps* mutant.

Primers for *manC* mutant construction were designed from the known *K. pneumoniae* K2 gene cluster sequence (Arakawa *et al*. 1995). Primer pairs ManCUPF (5'-CGCTTAAAGACCAGCGTGTCG -3'), ManCUPR (5´-CGGATCCGATCAGCGGGTCGTCGCCGTG_____-3'), and ManCDOWNF (5´-CGGATCCGCAGCGACGAGAAGCTGGTGG-3' *BamH*I site underlined), ManCDOWNR (5'-GGATATCCCGCAGGCCGGTG -3') were used in two sets of asymmetric PCRs to obtain DNA fragments ManCUP and ManCDown, respectively. DNA fragments ManCUP and ManCDOWN were annealed at their overlapping region and amplified by PCR as a single fragment using primers ManCUPF and ManCDOWNR. This PCR fragment was cloned into pGEM-T Easy to obtain pGEMTΔ*manC*. A kanamycin cassette, obtained as a 1.5 kb PCR fragment from pKD4 (Datsenko and Wanner. 2000) using primers cassette-F1 (5'-CGCGGATCCGTGTAGGCTGGAGCTGCTTCG-3' *BamH*I site underlined) and cassette-R1 (5'-CGCGGATCCCATGGGAATTAGCCATGGTCC -3' *BamH*I site underlined), was BamHI-

digested and cloned into BamHI-digested pGEMTΔ*manC* to obtain pGEMTΔ*manCKm*. Primers ManCUPF and ManCDOWNR were used to amplify a 3.5 kb fragment which was electroprated into Kp43816R containing pKOBEG-*sacB* plasmid (Derbise *et al*. 2003). The vector pKOBEG-*sacB* contains the Red operon expressed under the control of the arabinose inducible pBAD promoter and the *sacB* gene that is necessary to cure the plasmid. A recombinant in which the wild-type allele was replaced by Δ*man::Km* was verified by PCR and named 43Δ*manCKm*. The mutant was resistant to the CPS-specific phage ϕ2.

Eukaryotic cells culture.

Murine alveolar macrophages MH-S (ATCC, CRL-2019) and human monocytes THP-1 (ATCC, TIB-202) were grown in RPMI 1640 tissue culture medium supplemented with 10% heat-inactivated fetal calf serum (FCS) and 10 mM Hepes at 37ºC in an humidified 5% CO_2 atmosphere. THP-1 cells were differentiated to macrophages by PMA-treatment (10 ng/ml for 12 h).

Infection of macrophages.

Macrophages were seeded in 24-well tissue culture plates at a density of 7 x 10^5 cells per well 15 h before the experiment. Bacteria were grown in 5-ml LB, harvested in the exponential phase (2500 *x g*, 20 min, 24ºC), washed once with PBS and a suspension containing approximately 1x10^9 cfu/ml was prepared in 10 mM PBS (pH 6.5). Cells were infected with 35 µl of this suspension to get a multiplicity of infection of 50:1 in a final volume of 500 µl RPMI 1640 tissue culture medium supplemented with 10% heat-inactivated FCS and 10 mM Hepes. To synchronize infection, plates were centrifuged at 200 x *g* during 5 min. Plates were incubated at 37ºC in a humidified 5% CO_2 atmosphere. After 30 min of contact, cells were washed twice with PBS and incubated for additional 90 min with 500 µl RPMI 1640 containing 10% FCS, 10 mM Hepes, gentamicin (300 µg/ml) and polymyxin B (15 µg/ml) to eliminate extracellular bacteria. This treatment did not induce any cytotoxic effect which was verified measuring the release of lactate dehydrogenase (LDH) and by immunofluorescence microscopy (data not shown). For time course

experiments, after the 90 min treatment period, cells were washed three times with PBS and incubated with 500 µl RPMI 1640 containing 10% FCS, 10 mM Hepes, gentamicin (100 µg/ml).

To determine intracellular bacterial load, cells were washed three times with PBS and lysed with 300 µl of 0.5% saponin in PBS for 10 min at room temperature. Serial dilutions were plated on LB to quantify the number of intracellular bacteria. Intracellular bacterial load is represented as cfu per well. All experiments were done with triplicate samples on at least three independent occasions.

When indicated, cells were pre-incubated for 1 h with nocodazole (50 µg/ml), filipin (5 µg/ml), nystatin (25 µg/ml), LY294002 hydrochloride (75µM), or for 30 min with cytochalasin D (5 µg/ml) before carrying out infections as described above. Cells were also pre-incubated for 1 h with 1 mM methyl-β-cyclodextrin (MβCD), washed twice with PBS to remove cholesterol and infected. In other experiments, LY294002 hydrochloride (75µM), AKT X (10 µM), or 100 nM bafilomycin A_1 were added to the cells during the gentamicin treatment and kept until the end of experiment. Exposure to these drugs had no effect on cell and bacterial viability under the conditions tested. All drugs were purchased from Sigma.

Immunofluorescence and transmission electron microscopy.

Cells were seeded on 12 mm circular coverslips in 24-well tissue culture plates. Infections were carried out as described before with *K. pneumoniae* strains harbouring pFPV25.1Cm (March *et al*. 2013). Control experiments showed that there were no differences in the number of intracellular bacteria recovered over time from cells infected with bacteria containing pFPV25.1Cm or no plasmid (data not shown). When indicated, cells were washed three times with PBS and fixed with 3% paraformaldehyde (PFA) in PBS pH 7.4 for 15 min at room temperature. For EEA1 staining, cells were fixed with 2.5% PFA for 10 min at room temperature followed by 5% PFA + methanol (1:4 v/v) at -20°C for 5 min. Methanol fixation (3% PFA for 20 min at room temperature followed by 1 min cold methanol) was used for cathepsin D whereas periodate-lysine-paraformaldehyde fixation (0.01 M $NaIO_4$, 0.075 M L-lysine, 0.0375 M $NaPO_4$ buffer pH 7.4, 2% paraformaldehyde: 20 min room temperature) was used for calnexin. The actin cytoskeleton was

stained with Rhodamine-Phalloidin (Invitrogen) diluted 1:100, DNA was stained with Hoecsht 33342 (Invitrogen) diluted 1:2500. *Klebsiella* was stained with rabbit anti-*Klebsiella* serum diluted 1:5000. Early endosomes were stained with goat anti-EEA1 (N-19) antibody (Santa Cruz Biotechnology) diluted 1:50. Late endosomes were stained with rat anti-Lamp-1 (1D4B) antibody (Developmental Studies Hybridoma Bank). Lysosomes were labelled with goat anti-human cathepsin D (G19) or rabbit anti-human cathepsin D (H-75) antibodies (Santa Cruz Biotechnology) diluted 1:100. Golgi network was stained with mouse anti-GM130 (BD Laboratories) diluted 1:400. Endoplasmic reticulum was stained with rabbit anti-calnexin (SPA-860; Enzo Life Sciences) diluted 1:400. Donkey anti-rabbit, donkey anti-mouse, donkey anti-rat and donkey anti-goat conjugated to Rhodamine, Cy5 or Cy2 secondary antibodies were purchased from Jackson Immunological and diluted 1:200. Donkey anti-rabbit conjugated to AlexFluor 595 and goat anti-rabbit conjugated to Cascade blue antibodies (Life technologies) were diluted 1:200.

Fixable dextran 70,000 (molecular weight) labelled with Texas red (TR-dextran) (Molecular Probes) was used to label lysosomes in a pulse-chase assay. Briefly, macrophages seeded on glass coverslips were labelled by pulsing with 250 μg/ml of TR-dextran for 2 h at 37ºC in 5% CO_2 in RPMI 1640 medium. To allow TR-dextran to accumulate in lysosomes, medium was removed; cells were washed three times with PBS, and incubated for 1 h in dye-free medium (chase). After the chase period, cells were infected.

LysoTracker Red DND-99 (Invitrogen) was used to label acidic organelles following the instructions of the manufacturer. 0.5 μM Lysotracker RedDN99 was added to the tissue culture medium 30 min before fixing the cells. The residual fluid marker was removed by washing the cells three times with PBS, followed by fixation.

Staining was carried out in 10% horse serum, 0.1% saponin in PBS. Coverslips were washed twice in PBS containing 0.1% saponin, once in PBS, and incubated for 30 minutes with primary antibodies. Coverslips were then washed twice in 0.1% saponin in PBS and once in PBS and incubated for 30 minutes with secondary antibodies. Finally, coverslips were washed twice in 0.1%

saponin in PBS, once in PBS and once in H_2O, mounted on Aqua Poly/Mount (Polysciences). Immunofluorescence was analysed with a Leica CTR6000 fluorescence microscope. Images were taken with a Leica DFC350FX monochrome camera. Confocal microscopy was carried out with a Leica TCS SP5 confocal microscope. Depending of the marker, a KCV was considered positive when it fulfilled these criteria: (i) the marker was detected throughout the area occupied by the bacterium; (ii) the marker was detected around/enclosing the bacterium, (iii) the marker was concentrated in this area, compared to the immediate surroundings. To determine the percentage of bacteria that colocalized with each marker, all bacteria located inside a minimum of 100 infected cells were analysed in each experiment. Experiments were carried out by triplicate in three independent occasions.

For extra-/intracellular bacteria differential staining, PFA fixed cells were incubated with PBS containing 10% horse serum, Hoechst 33342 and rabbit anti-*Klebsiella* for 20 min. Coverslips were washed three times with PBS and stained as described above with donkey anti-rabbit conjugated to Rhodamine secondary antibody. Coverslips were washed three times in PBS and once in distilled water before mounting onto glass slides using Prolong Gold antifade mounting gel (Invitrogen).

For transmission electron microscopy (TEM), cells were seeded in 24-well tissue culture plates. Infections were carried out as described before, fixed with glutaraldehyde and processed for TEM as described previously (Kruskal *et al*. 1992).

Assessment of intracellular bacteria viability

(i) Fluorescent *in situ* hybridisation

We carried out hybridization of PFA fixed infected cells with fluorescently labelled oligonucleotides as described before (Morey *et al*. 2011). Alexa488 conjugated DNA probes EUB338 (5'-GCTGCCTCCCGTAGGAGT-3') and GAM42a (5'-GCCTTCCCACATCGTTT-3') were designed for specific labelling of rRNA of eubacteria and gamma subclass of Proteobacteria, respectively (Manz *et al*. 1993). A DNA probe non-EUB338, complementary to EUB338 was used

as a negative control. The detectability of bacteria by such oligonucleotide probes is dependent on the presence of sufficient ribosomes per cell, hence providing qualitative information on the physiological state of the bacteria on the basis of the number of ribosomes per cell. These probes were used together to obtain a stronger signal, added to a final concentration of 5 nM each in the hybridation buffer. The hybridization buffer contained 0.9M NaCl, 20mM Tris-HCl (pH 7.4), 0.01% sodium dodecyl sulfate (SDS) and 35% formamide. Coverslips were first washed with deionized water. Hybridization was carried out for 1.5 h at 46ºC in a humid chamber; followed by a 30 min wash at 48ºC. Washing buffer contained 80 mM NaCl, 20 mM Tris-HCl (pH 7.4), 0.01% sodium dodecyl sulfate (SDS) and 5 mM EDTA (pH 8). After washing, DNA staining for total bacteria was carried out by incubating the coverslips in PBS containing Hoechst 33342 for 20 min. Coverslips were then washed three times in PBS and once in distilled water before mounting onto glass slides using Prolong Gold antifade mounting gel.

(ii) Two fluorescent markers tagging

pJT04mCherry, expressing mCherry constituvely (kindly donated by Miguel Valvano, to be described elsewhere), and pMMB207gfp3.1 (Pujol *et al*. 2005), expressing *gfpmut3.1* under the control of an IPTG-inducible promoter, were conjugated into Kp43816R. Control experiments confirmed that UV-killed *Klebsiella* was always mCherry positive and GFP negative whereas live *Klebsiella* was mCherry positive and only GFP positive if IPTG was added (1 mM, 1.5 h) to the medium. Cells were infected with Kp43816R harbouring both plasmids and IPTG was added to the medium 1.5 h before fixing the cells with PFA. To stain extracellular bacteria, PFA fixed cells were incubated with PBS containing 10% horse serum, and rabbit anti-*Klebsiella* for 20 min. Coverslips were washed three times with PBS and stained as described above with goat anti-rabbit antibodies conjugated to Cascade Blue (C2764, Life Technologies). Immunofluorescence was analysed with a Leica CTR6000 fluorescence microscope. Images were taken with a Leica DFC350FX monochrome camera.

Isolation of *in vivo* infected macrophages

644 Mice were treated in accordance with the Directive of the European Parliament and of the
645 Council on the protection of animals used for scientific purposes (Directive 2010/63/EU) and in
646 agreement with the UK Home Office (licence PLZ 2700) and the Bioethical Committee of the
647 University of the Balearic Islands (authorisation number 1748).

648 Infections were performed as previously described (Insua *et al*. 2013). Briefly, five- to
649 seven-week-old male C57BL/6 mice (Harlan) were anesthetized by intraperitoneal injection with a
650 mixture containing ketamine (50 mg/kg) and xylazine (5 mg/kg). Overnight bacterial cultures were
651 centrifuged (2500 x g, 20 min, 22ºC), resuspended in PBS and adjusted to 5 x 10^4 CFU/ml for
652 determination of bacterial loads. 20 µl of the bacterial suspension were inoculated intranasally in
653 four 5 µl aliquots. To facilitate consistent inoculations, mice were held vertically during inoculation
654 and placed on a 45° incline while recovering from anaesthesia. 24 h post infection, mice were
655 euthanized by cervical dislocation and bronchoalveolar lavage was performed as previously
656 described (Cai *et al*. 2012). The lavage fluid from four mice was pooled together and spun at 300 *x*
657 g for 10 min to pellet alveolar macrophages. Cells were cultured on 12 mm circular coverslips in
658 24-well tissue culture plates at a concentration of 0.5 x 10^6 cells/well in 1 ml RPMI 1640 tissue
659 culture medium supplemented with 10% heat-inactivated FCS and 10 mM Hepes and gentamicin
660 (100 µg/ml). After 2 h of incubation, nonadherent cells were washed off with PBS, and cells were
661 fixed. Cathepsin D staining was performed as previously described. To label lysosomes using TR-
662 dextran, after washing off the nonadherent cells, the attached macrophages were pulsed with TR-
663 dextran (250 µg/ml) for 2 h in RPMI 1640 medium containing gentamicin (100 µg/ml). Cells were
664 washed three times with PBS, and incubated for 1 h in dye-free medium (chase). After the chase
665 period, cells were fixed. Immunofluorescence was analysed with a Leica TCS SP5 confocal
666 microscope.

667 **Neutral red uptake assay for the estimation of cell viability.**

668 Cell viability was determined by assessing the ability of viable cells to incorporate and bind
669 the supravital dye neutral red in the lysosomes. The protocol described by Repetto and coworkers

(Repetto *et al*. 2008) was followed with minor modifications. Macrophages were seeded on 96-well tissue culture plates at 5 x 10^5 cells/well 18 h before the experiment. Cells were infected to get a multiplicity of infection of 50:1 in a final volume of 200 µl RPMI 1640 tissue culture medium supplemented with 10% heat-inactivated FCS and 10 mM Hepes. To synchronize infection, plates were centrifuged at 200 x *g* during 5 min. Plates were incubated at 37ºC in a humidified 5% CO_2 atmosphere. After 90 min of contact, cells were washed twice with PBS and incubated overnight with 200 µl RPMI 1640 containing 10% FCS, 10 mM Hepes, gentamicin (100 µg/ml). Cells were washed twice with PBS and incubated with 100 µl of freshly prepared neutral red medium (final concentration 40 µg/ml neutral red [Sigma] in tissue culture medium) for 2 h. Wells were washed once with PBS and the remaining biomass-adsorbed neutral red was solubilized with 150 µl neutral red destaining solution (50% ethanol 96%; 49% deionised water, 1% glacial acetic acid). Staining was then quantified by determining the OD_{540} in a 96-well microplate reader, and used to compare relative neutral red staining of uninfected cells and cells that were lysed completely with 1% Triton X-100. Experiments were carried out by triplicate in six independent occasions.

Detection of Akt phosphorylation by Western blotting

Macrophages were seeded on 6-well tissue culture plates at 10^6 cells/well. Cells were infected with Kp43816R , washed 3 times with cold PBS, scraped and lysed with 100 µl lysis buffer (1x SDS Sample Buffer, 62.5 mM Tris-HCl pH 6.8, 2% w/v SDS, 10% glycerol, 50 mM DTT, 0.01% w/v bromophenol blue) on ice. Samples were sonicated, boiled at 100ºC for 10 min and cooled on ice before polyacrylamide gel electrophoresis and Western Blotting. Akt phosphorylation was detected with primary rabbit anti-phospho Ser473 Akt (Cell Signaling Technology) antibody diluted 1:1,000 and secondary goat anti-rabbit antibody conjugated to horseradish peroxidase (Thermo Scientific) diluted 1:10,000. Tubulin was detected with primary mouse anti-tubulin antibody (Sigma) diluted 1:3,000 and secondary goat anti-mouse antibody (Pierce) conjugated to horseradish peroxidase diluted 1:1,000. To detect tubulin, membranes were reprobed after stripping

of previously used antibodies using Western Blot Stripping Buffer (Thermo Scientific). Images were recorded with a GeneGnome HR imaging system (Syngene).

Apoptosis analysis *in vitro*.

Apoptosis of macrophages was analysed as previously described (Aguilo *et al*. 2013). Briefly, phosphatydylserine exposure and membrane integrity were analyzed by using Annexin-V and 7-AAD (BD Biosciences) and FACS according to manufacturer instructions. Cells were washed with PBS and incubated with APC-conjugated Annexin-V and 7-AAD in Annexin-binding buffer for 15 min. After that, cells were washed twice with PBS, fixed with 4% PFA during 30 min and washed again with PBS. Both PBS and PFA contained 2.5 mM $CaCl_2$.

Bacterial opsonisation.

Normal human serum (NHS), kindly donated by the Balearics Blood Centre, was obtained from five different donors (blood type O negative) and kept frozen at -80^{o}C. 35 µl from a suspension containing approximately 1x10^{9} cfu/ml in 10 mM PBS (pH 6.5) were added to 500 µl RPMI 1640 tissue culture medium supplemented with 10 mM Hepes and 1% NHS. The suspension was incubated at 37^{o}C shaking (180 rpm) for 45 min. The suspension was used to infect mTHP1 cells as previously described.

Plasmids and transient transfections

For transient transfections with GFP-Rab7 (Addgene plasmid #28047) (Sun *et al*. 2010), GFP-Rab14 (Kuijl *et al*. 2007), and RILP-C33-EGFP (Cantalupo *et al*. 2001), the Neon transfection system was used (Life Technologies). 8 x 10^{6} cells were transfected (1400 v, 30 ms and 1 pulse) with 2 µg of plasmid DNA. After, cells were seeded on 12 mm circular coverslips in 24-well tissue culture plates and 24 h later were infected. In all cases, samples were fixed, stained and analysed by immunofluorescence microscopy. pcDNA3 and DN-Rab14 (Seto *et al*. 2011) were transfected using jetPEI-macrophage (Polyplus) following manufacturer´s instructions. After 24 h, cells were washed twice with PBS, infected, and intracellular bacterial load determined as previously described.

Construction of *cps* reporter strain

DNA fragment containing the promoter region of the Kp43816R capsule operon was amplified by PCR using *Vent* polymerase (NewEngland Biolabs) and primers K2ProcpsF (5'-gaattcTGCTGGGACAAATTGCCACC-3') and K2ProcpsR (5'-AGATGGATGACCCCGCGATC-3'). To construct a green fluorescent protein (GFP) reporter, the PCR product was EcoRI-digested and cloned into the EcoRI-SmaI digested low-copy-number vector pPROBE'-gfp[LVA] (Miller *et al*. 2000) to obtain pPROBE'43Procps. The plasmid was introduced into Kp43816R by electroporation.

Analysis of *cps* expression

The reporter strain was grown at 37ºC on an orbital incubator shaker (180 r.p.m.) until OD_{540} 1.2. The cultures were harvested (2500 x g, 20 min, 24ºC) and resuspended to an OD_{540} of 0.6 in PBS. 0.8-ml aliquot of this suspension was transferred to 1-cm fluorimetric cuvette and fluorescence was measured with a spectrofluorophotomoter (Perkin Elmer LS55) set as follows: excitation, 485 nm; emission, 528 nm; slit width 5 nm; integration time 5 seconds. Results were expressed as relative fluorescence units (RFU). All measurements were carried out in quintuplicate on at least three separate occasions.

To obtain RNA, bacteria were grown at 37^{o}C in 5 ml of medium on an orbital incubator shaker (180 r.p.m.) until an OD_{600} of 0.3. 3 ml of RNA later solution were added to the culture and the mixture was incubated for 20 min to prevent RNA degradation. Total RNA was extracted using Trizol as recommended by the manufacturer (Life Technology). The purification included a DNAase treatment step. cDNA was obtained by retrotranscription of 1 µg of total RNA using a commercial M-MLV Reverse Transcriptase (Sigma), and random primers mixture (Invitrogen). 20 ng of cDNA were used as a template in a 10-µl reaction. RT-PCR analyses were performed with a Mx3005P qPCR System (Agilent Technologies) and using a KapaSYBR Fast qPCR Kit as recommended by the manufacturer (Kapa biosystems). The thermocycling protocol was as follows; 95°C for 3 min for hot-start polymerase activation, followed by 40 cycles of 95°C for 10 s, and

56°C for 20 s. SYBR green dye fluorescence was measured at 521 nm. cDNAs were obtained from two independent extractions of mRNA and each one amplified by RT-qPCR in two independent occasions. Relative quantities of *wzi*, *orf7* and *gnd* mRNAs were obtained using the comparative threshold cycle (ΔΔCT) method by normalizing to *rpoD* gene. Primers used were: Kpn_RpoD_F1 (5'-CCGGAAGACAAAATCCGTAA-3') and Kpn_RpoD_R1 (5'-CGGGTAACGTCGAACTGTTT-3'); Kp43/52_wzi_F2 (5'-TCGACCGCAATCATTCAGCA-3') and Kp43/52_wzi_R2 (5'-CATCCTTACCCCAGCCGTG-3'); Kp43/52_orf7_F1 (5'-ATCAAGATTGCCGACGTTTCT-3') and Kp43/52_orf7_R1 (5'-GCCTCTACCGCAACTAATCCA-3'); Kp43/52_gnd_F1 (5'-GGATC CGGCGAACCTCTTT-3') and Kp43/52_gnd_R1 (5'-GCCCTGAGCATAGGAAACGA-3').

For analysis of *cps* expression from intracellular bacteria, macrophages were seeded in 6-well plates and infected with Kp43816R containing pPROBE'43Procps or pPROBE'-gfp[LVA] control vector at a MOI of 150:1. After 40 min, cells were washed twice with PBS and incubated with 500 µl RPMI 1640 containing 10% FCS, 10 mM Hepes, gentamicin (300 µg/ml) and polymyxin B (15 µg/ml) to eliminate extracellular bacteria. At the indicated time points, cells were lysed with 900 µl 0.5 % saponin in PBS. The samples from two wells were combined and serial dilutions were plated on LB to quantify the number of intracellular bacteria. Control experiments showed that there were no differences in the number of intracellular bacteria recovered over time from cells infected with bacteria containing pPROBE'-gfp[LVA] derivatives or no plasmid (data not shown). By replica plating on plates containing kanamycin, it was determined that 85-100% of the bacteria contained the reporter plasmid at any time point analysed. The rest of the lysate was centrifuged (13 000 rpm, 1 min, room temperature) and resuspended in 1 ml 1 % BSA in PBS for staining. Bacteria were stained with rabbit anti-*Klebsiella* serum diluted 1:5000 for 20 min, washed twice with PBS, and incubated for 20 min with a 1:200 dilution of Rhodamine-conjugated donkey anti-rabbit secondary antibody. Flow cytometry analyses were performed using a Cultek Epics XL flow cytometer. Samples were gated for bacteria-like particles by using the rhodamine fluorescence

of the anti-*Klebsiella* labelling to identify bacterial cells and to exclude mammalian cell debris and background noise. Lysed and stained uninfected macrophages were not rhodamine positive, indicating that there was no cross-reactivity of the primary or secondary antibodies with MH-S cells. Fluorescence compensation settings were determined in parallel under identical conditions by using the constitutively GFP-expressing Kp43816R strain or the non-expressing strain, with and without anti-*Klebsiella* antibody labelling. Approximately 10,000 events identified as *Klebsiella* cells were collected per sample. A histogram of GFP fluorescence for the negative-control sample (bacteria containing pPROBE'-gfp[LVA]) was created, and the area of the histogram containing the bacterial population was considered to be negative for GFP fluorescence. All experiments were done with triplicate samples on at least three independent occasions.

Statistical analysis.

Statistical analyses were performed using the one-tailed *t* test or, when the requirements were not met, by the Mann-Whitney U test. $P < 0.05$ was considered statistically significant. The analyses were performed using Prism4 for PC (GraphPad Software).

ACKNOWLEDGEMENTS

We are grateful to members of Bengoechea lab for helpful discussions. We are indebted to Miguel Valvano, Sergio Grinstein, Jacques Neefjes, Jim Bliska and Yukio Koide for sending us plasmids and helpful discussions. M.I.M.-L. was financially supported by the Instituto de Salud Carlos III (grant CM09/000123). Part of this work was supported by grant PS09-00130 from Instituto de Salud Carlos III to J.G., and by grants from Biomedicine Program (SAF2009-07885 and SAF2012-39841) from Ministerio de Economía y Competitividad (Spain), Govern Illes Balears (Competitive group Ref: 46/2011); and Queen's University Belfast start-up funds to J.A.B. This research was also supported by a Marie Curie FP7 Integration Grant (U-KARE; PCIG13-GA-2013-618162) to J.A.B. within the 7th European Union Framework Programme. CIBERES is an initiative from Instituto de Salud Carlos III.

REFERENCES

Aderem, A., and Underhill, D.M. (1999) Mechanisms of phagocytosis in macrophages. *Annu Rev Immunol* 17: 593-623.

Aguilo, J.I., Alonso, H., Uranga, S., Marinova, D., Arbues, A., de Martino, A., *et al* (2013) ESX-1-induced apoptosis is involved in cell-to-cell spread of *Mycobacterium tuberculosis*. *Cell Microbiol* 15: 1994-2005.

Alvarez, D., Merino, S., Tomas, J.M., Benedi, V.J., and Alberti, S. (2000) Capsular polysaccharide is a major complement resistance factor in lipopolysaccharide O side chain-deficient *Klebsiella pneumoniae* clinical isolates. *Infect Immun* 68: 953-955.

Arakawa, Y., Wacharotayankun, R., Nagatsuka, T., Ito, H., Kato, N., and Ohta, M. (1995) Genomic organization of the *Klebsiella pneumoniae cps* region responsible for serotype K2 capsular polysaccharide synthesis in the virulent strain Chedid. *J Bacteriol* 177: 1788-1796.

Bakker-Woudenberg, I.A., van den Berg J.C., Vree T.B., Baars A.M., and Michel M.F. (1985) Relevance of serum protein binding of cefoxitin and cefazolin to their activities against *Klebsiella pneumoniae* pneumonia in rats. Antimicrob Agents Chemother 28:654-659.

Broug-Holub, E., Toews, G.B., van Iwaarden, J.F., Strieter, R.M., Kunkel, S.L., Paine, R.,3rd, *et al* (1997) Alveolar macrophages are required for protective pulmonary defenses in murine *Klebsiella* pneumonia: elimination of alveolar macrophages increases neutrophil recruitment but decreases bacterial clearance and survival. *Infect Immun* 65: 1139-1146.

Cai, S., Batra, S., Wakamatsu, N., Pacher, P., and Jeyaseelan, S. (2012) NLRC4 inflammasome-mediated production of IL-1beta modulates mucosal immunity in the lung against gram-negative bacterial infection. *J Immunol* 188: 5623-5635.

Campos, M.A., Vargas, M.A., Regueiro, V., Llompart, C.M., Alberti, S., and Bengoechea, J.A. (2004) Capsule polysaccharide mediates bacterial resistance to antimicrobial peptides. *Infect Immun* 72: 7107-7114.

Camprubi, S., Merino, S., Benedi, V.J., and Tomas, J.M. (1993) The role of the O-antigen lipopolysaccharide and capsule on an experimental *Klebsiella pneumoniae* infection of the rat urinary tract. *FEMS Microbiol Lett* 111: 9-13.

Cano, V., Moranta, D., Llobet-Brossa, E., Bengoechea, J.A., and Garmendia, J. (2009) *Klebsiella pneumoniae* triggers a cytotoxic effect on airway epithelial cells. *BMC Microbiol* 9: 156-2180-9-156.

Cantalupo, G., Alifano, P., Roberti, V., Bruni, C.B., and Bucci, C. (2001) Rab-interacting lysosomal protein (RILP): the Rab7 effector required for transport to lysosomes. *EMBO J* 20: 683-693.

Cheung, D.O., Halsey, K., and Speert, D.P. (2000) Role of pulmonary alveolar macrophages in defense of the lung against *Pseudomonas aeruginosa*. *Infect Immun* 68: 4585-4592.

Chiu, H.C., Soni, S., Kulp, S.K., Curry, H., Wang, D., Gunn, J.S., *et al* (2009) Eradication of intracellular *Francisella tularensis* in THP-1 human macrophages with a novel autophagy inducing agent. *J Biomed Sci* 16: 110-0127-16-110.

Christensen, H., Hansen, M., and Sorensen, J. (1999) Counting and size classification of active soil bacteria by fluorescence in situ hybridization with an rRNA oligonucleotide probe. *Appl Environ Microbiol* 65: 1753-1761.

Cortes, G., Alvarez, D., Saus, C., and Alberti, S. (2002a) Role of lung epithelial cells in defense against *Klebsiella pneumoniae* pneumonia. *Infect Immun* 70: 1075-1080.

Cortes, G., Borrell, N., de Astorza, B., Gomez, C., Sauleda, J., and Alberti, S. (2002b) Molecular analysis of the contribution of the capsular polysaccharide and the lipopolysaccharide O side chain to the virulence of *Klebsiella pneumoniae* in a murine model of pneumonia. *Infect Immun* 70: 2583-2590.

Datsenko, K.A., and Wanner, B.L. (2000) One-step inactivation of chromosomal genes in Escherichia coli K-12 using PCR products. *Proc Natl Acad Sci U S A* 97: 6640-6645.

de Astorza, B., Cortes, G., Crespi, C., Saus, C., Rojo, J.M., and Alberti, S. (2004) C3 promotes clearance of *Klebsiella pneumoniae* by A549 epithelial cells. *Infect Immun* 72: 1767-1774.

Derbise, A., Lesic, B., Dacheux, D., Ghigo, J.M., and Carniel, E. (2003) A rapid and simple method for inactivating chromosomal genes in *Yersinia*. *FEMS Immunol Med Microbiol* 38: 113-116.

Drecktrah, D., Knodler, L.A., Ireland, R., and Steele-Mortimer, O. (2006) The mechanism of *Salmonella* entry determines the vacuolar environment and intracellular gene expression. *Traffic* 7: 39-51.

Drevets, D.A., Leenen, P.J., and Campbell, P.A. (1993) Complement receptor type 3 (CD11b/CD18) involvement is essential for killing of *Listeria monocytogenes* by mouse macrophages. *J Immunol* 151: 5431-5439.

Eissenberg, L.G., Schlesinger, P.H., and Goldman, W.E. (1988) Phagosome-lysosome fusion in P388D1 macrophages infected with *Histoplasma capsulatum*. *J Leukoc Biol* 43: 483-491.

Fevre, C., Almeida, A.S., Taront, S., Pedron, T., Huerre, M., Prevost, M.C., *et al* (2013) A novel murine model of rhinoscleroma identifies Mikulicz cells, the disease signature, as IL-10 dependent derivatives of inflammatory monocytes. *EMBO Mol Med* 5: 516-530.

Fink, S.L., and Cookson, B.T. (2007) Pyroptosis and host cell death responses during *Salmonella* infection. *Cell Microbiol* 9: 2562-2570.

Finlay, B.B., and McFadden, G. (2006) Anti-immunology: evasion of the host immune system by bacterial and viral pathogens. *Cell* 124: 767-782.

Flannagan, R.S., Cosio, G., and Grinstein, S. (2009) Antimicrobial mechanisms of phagocytes and bacterial evasion strategies. *Nat Rev Microbiol* 7: 355-366.

Flannagan, R.S., Jaumouille, V., and Grinstein, S. (2012) The cell biology of phagocytosis. *Annu Rev Pathol* 7: 61-98.

Fortier, A.H., Leiby, D.A., Narayanan, R.B., Asafoadjei, E., Crawford, R.M., Nacy, C.A., *et al* (1995) Growth of *Francisella tularensis* LVS in macrophages: the acidic intracellular compartment provides essential iron required for growth. *Infect Immun* 63: 1478-1483.

Frank, C.G., Reguerio, V., Rother, M., Moranta, D., Maeurer, A.P., Garmendia, J., *et al* (2013) *Klebsiella pneumoniae* targets an EGF receptor-dependent pathway to subvert inflammation. *Cell Microbiol* 15: 1212-1233.

Garcia-del Portillo, F., Foster, J.W., Maguire, M.E., and Finlay, B.B. (1992) Characterization of the micro-environment of *Salmonella typhimurium*-containing vacuoles within MDCK epithelial cells. *Mol Microbiol* 6: 3289-3297.

Geier, H., and Celli, J. (2011) Phagocytic receptors dictate phagosomal escape and intracellular proliferation of *Francisella tularensis*. *Infect Immun* 79: 2204-2214.

Ghigo, E., Capo, C., Aurouze, M., Tung, C.H., Gorvel, J.P., Raoult, D., *et al* (2002) Survival of *Tropheryma whipplei*, the agent of Whipple's disease, requires phagosome acidification. *Infect Immun* 70: 1501-1506.

Gordon, S.B., Irving, G.R., Lawson, R.A., Lee, M.E., and Read, R.C. (2000) Intracellular trafficking and killing of *Streptococcus pneumoniae* by human alveolar macrophages are influenced by opsonins. *Infect Immun* 68: 2286-2293.

Greco, E., Quintiliani, G., Santucci, M.B., Serafino, A., Ciccaglione, A.R., Marcantonio, C., *et al* (2012) Janus-faced liposomes enhance antimicrobial innate immune response in *Mycobacterium tuberculosis* infection. *Proc Natl Acad Sci U S A* 109: E1360-8.

Greenberger, M.J., Kunkel, S.L., Strieter, R.M., Lukacs, N.W., Bramson, J., Gauldie, J., *et al* (1996a) IL-12 gene therapy protects mice in lethal *Klebsiella* pneumonia. *J Immunol* 157: 3006-3012.

Greenberger, M.J., Strieter, R.M., Kunkel, S.L., Danforth, J.M., Laichalk, L.L., McGillicuddy, D.C., *et al* (1996b) Neutralization of macrophage inflammatory protein-2 attenuates neutrophil recruitment and bacterial clearance in murine *Klebsiella* pneumonia. *J Infect Dis* 173: 159-165.

Happel, K.I., Dubin, P.J., Zheng, M., Ghilardi, N., Lockhart, C., Quinton, L.J., *et al* (2005) Divergent roles of IL-23 and IL-12 in host defense against *Klebsiella pneumoniae*. *J Exp Med* 202: 761-769.

Happel, K.I., Zheng, M., Young, E., Quinton, L.J., Lockhart, E., Ramsay, A.J., *et al* (2003) Cutting edge: roles of Toll-like receptor 4 and IL-23 in IL-17 expression in response to *Klebsiella pneumoniae* infection. *J Immunol* 170: 4432-4436.

Hilbi, H., Moss, J.E., Hersh, D., Chen, Y., Arondel, J., Banerjee, S., *et al* (1998) *Shigella*-induced apoptosis is dependent on caspase-1 which binds to IpaB. *J Biol Chem* 273: 32895-32900.

Hmama, Z., Sendide, K., Talal, A., Garcia, R., Dobos, K., and Reiner, N.E. (2004) Quantitative analysis of phagolysosome fusion in intact cells: inhibition by mycobacterial lipoarabinomannan and rescue by an 1alpha,25-dihydroxyvitamin D3-phosphoinositide 3-kinase pathway. *J Cell Sci* 117: 2131-2140.

Hoogendijk, A.J., Diks, S.H., Peppelenbosch, M.P., Van Der Poll, T., and Wieland, C.W. (2011) Kinase activity profiling of gram-negative pneumonia. *Mol Med* 17: 741-747.

Howe, D., and Mallavia, L.P. (2000) *Coxiella burnetii* exhibits morphological change and delays phagolysosomal fusion after internalization by J774A.1 cells. *Infect Immun* 68: 3815-3821.

Insua, J.L., Llobet, E., Moranta, D., Perez-Gutierrez, C., Tomas, A., Garmendia, J., *et al* (2013) Modelling *Klebsiella pneumoniae* pathogenesis by infecting the wax moth *Galleria mellonella*. *Infect Immun*. 81: 3552-3565.

Jordens, I., Fernandez-Borja, M., Marsman, M., Dusseljee, S., Janssen, L., Calafat, J., *et al* (2001) The Rab7 effector protein RILP controls lysosomal transport by inducing the recruitment of dynein-dynactin motors. *Curr Biol* 11: 1680-1685.

Krachler, A.M., Woolery, A.R., and Orth, K. (2011) Manipulation of kinase signaling by bacterial pathogens. *J Cell Biol* 195: 1083-1092.

Kruskal, B.A., Sastry, K., Warner, A.B., Mathieu, C.E., and Ezekowitz, R.A. (1992) Phagocytic chimeric receptors require both transmembrane and cytoplasmic domains from the mannose receptor. *J Exp Med* 176: 1673-1680.

Kuijl, C., Savage, N.D., Marsman, M., Tuin, A.W., Janssen, L., Egan, D.A., *et al* (2007) Intracellular bacterial growth is controlled by a kinase network around PKB/AKT1. *Nature* 450: 725-730.

Kyei, G.B., Vergne, I., Chua, J., Roberts, E., Harris, J., Junutula, J.R., *et al* (2006) Rab14 is critical for maintenance of *Mycobacterium tuberculosis* phagosome maturation arrest. *EMBO J* 25: 5250-5259.

Lamothe, J., Huynh, K.K., Grinstein, S., and Valvano, M.A. (2007) Intracellular survival of *Burkholderia cenocepacia* in macrophages is associated with a delay in the maturation of bacteria-containing vacuoles. *Cell Microbiol* 9: 40-53.

Lawlor, M.S., Handley, S.A., and Miller, V.L. (2006) Comparison of the host responses to wild-type and *cpsB* mutant *Klebsiella pneumoniae* infections. *Infect Immun* 74: 5402-5407.

Lawlor, M.S., Hsu, J., Rick, P.D., and Miller, V.L. (2005) Identification of *Klebsiella pneumoniae* virulence determinants using an intranasal infection model. *Mol Microbiol* 58: 1054-1073.

Manz, W., Szewzyk, U., Ericsson, P., Amann, R., Schleifer, K.H., and Stenstrom, T.A. (1993) In situ identification of bacteria in drinking water and adjoining biofilms by hybridization with 16S and 23S rRNA-directed fluorescent oligonucleotide probes. *Appl Environ Microbiol* 59: 2293-2298.

March, C., Cano, V., Moranta, D., Llobet, E., Perez-Gutierrez, C., Tomas, J.M., *et al* (2013) Role of bacterial surface structures on the interaction of *Klebsiella pneumoniae* with phagocytes. *PLoS One* 8: e56847.

Miller, W.G., Leveau, J.H., and Lindow, S.E. (2000) Improved *gfp* and *inaZ* broad-host-range promoter-probe vectors. *Mol Plant Microbe Interact* 13: 1243-1250.

Moranta, D., Regueiro, V., March, C., Llobet, E., Margareto, J., Larrarte, E., *et al* (2010) *Klebsiella pneumoniae* capsule polysaccharide impedes the expression of beta-defensins by airway epithelial cells. *Infect Immun* 78: 1135-1146.

Morey, P., Cano, V., Marti-Lliteras, P., Lopez-Gomez, A., Regueiro, V., Saus, C., *et al* (2011) Evidence for a non-replicative intracellular stage of nontypable *Haemophilus influenzae* in epithelial cells. *Microbiology* 157: 234-250.

Munoz-Price, L.S., Poirel, L., Bonomo, R.A., Schwaber, M.J., Daikos, G.L., Cormican, M., *et al* (2013) Clinical epidemiology of the global expansion of *Klebsiella pneumoniae* carbapenemases. *Lancet Infect Dis* 13: 785-796.

Navarre, W.W., and Zychlinsky, A. (2000) Pathogen-induced apoptosis of macrophages: a common end for different pathogenic strategies. *Cell Microbiol* 2: 265-273.

Oelschlaeger, T.A., and Tall, B.D. (1997) Invasion of cultured human epithelial cells by *Klebsiella pneumoniae* isolated from the urinary tract. *Infect Immun* 65: 2950-2958.

Porte, F., Liautard, J.P., and Kohler, S. (1999) Early acidification of phagosomes containing *Brucella suis* is essential for intracellular survival in murine macrophages. *Infect Immun* 67: 4041-4047.

Pujol, C., Grabenstein, J.P., Perry, R.D., and Bliska, J.B. (2005) Replication of *Yersinia pestis* in interferon gamma-activated macrophages requires ripA, a gene encoded in the pigmentation locus. *Proc Natl Acad Sci U S A* 102: 12909-12914.

Regueiro, V., Campos, M.A., Pons, J., Alberti, S., and Bengoechea, J.A. (2006) The uptake of a *Klebsiella pneumoniae* capsule polysaccharide mutant triggers an inflammatory response by human airway epithelial cells. *Microbiology* 152: 555-566.

Repetto, G., del Peso, A., and Zurita, J.L. (2008) Neutral red uptake assay for the estimation of cell viability/cytotoxicity. *Nat Protoc* 3: 1125-1131.

977 Rink, J., Ghigo, E., Kalaidzidis, Y., and Zerial, M. (2005) Rab conversion as a mechanism of
978 progression from early to late endosomes. *Cell* 122: 735-749.

979 Sahly, H., and Podschun, R. (1997) Clinical, bacteriological, and serological aspects of *Klebsiella*
980 infections and their spondylarthropathic sequelae. *Clin Diagn Lab Immunol* 4: 393-399.

981 Sarantis, H., and Grinstein, S. (2012) Subversion of phagocytosis for pathogen survival. *Cell Host*
982 *Microbe* 12: 419-431.

983 Seto, S., Tsujimura, K., and Koide, Y. (2011) Rab GTPases regulating phagosome maturation are
984 differentially recruited to mycobacterial phagosomes. *Traffic* 12: 407-420.

985 Smith, A.C., Heo, W.D., Braun, V., Jiang, X., Macrae, C., Casanova, J.E., *et al* (2007) A network
986 of Rab GTPases controls phagosome maturation and is modulated by *Salmonella enterica* serovar
987 Typhimurium. *J Cell Biol* 176: 263-268.

988 Sun, Q., Westphal, W., Wong, K.N., Tan, I., and Zhong, Q. (2010) Rubicon controls endosome
989 maturation as a Rab7 effector. *Proc Natl Acad Sci U S A* 107: 19338-19343.
990

991 Thi, E.P., and Reiner, N.E. (2012) Phosphatidylinositol 3-kinases and their roles in phagosome
992 maturation. *J Leukoc Biol* 92: 553-566.

993 Trombetta, E.S., and Mellman, I. (2005) Cell biology of antigen processing in vitro and in vivo.
994 *Annu Rev Immunol* 23: 975-1028.

995 Vieira, O.V., Botelho, R.J., and Grinstein, S. (2002) Phagosome maturation: aging gracefully.
996 *Biochem J* 366: 689-704.

997 Vieira, O.V., Botelho, R.J., Rameh, L., Brachmann, S.M., Matsuo, T., Davidson, H.W., *et al* (2001)
998 Distinct roles of class I and class III phosphatidylinositol 3-kinases in phagosome formation and
999 maturation. *J Cell Biol* 155: 19-25.

1000 von Bargen, K., Gorvel, J.P., and Salcedo, S.P. (2012) Internal affairs: investigating the *Brucella*
1001 intracellular lifestyle. *FEMS Microbiol Rev* 36: 533-562.

1002 Willingham, S.B., Allen, I.C., Bergstralh, D.T., Brickey, W.J., Huang, M.T., Taxman, D.J., *et al*
1003 (2009) NLRP3 (NALP3, Cryopyrin) facilitates in vivo caspase-1 activation, necrosis, and HMGB1
1004 release via inflammasome-dependent and -independent pathways. *J Immunol* 183: 2008-2015.

1005 Willingham, S.B., Bergstralh, D.T., O'Connor, W., Morrison, A.C., Taxman, D.J., Duncan, J.A., *et*
1006 *al* (2007) Microbial pathogen-induced necrotic cell death mediated by the inflammasome
1007 components CIAS1/cryopyrin/NLRP3 and ASC. *Cell Host Microbe* 2: 147-159.

1008 Wu, J., Kobayashi, M., Sousa, E.A., Liu, W., Cai, J., Goldman, S.J., *et al* (2005) Differential
1009 proteomic analysis of bronchoalveolar lavage fluid in asthmatics following segmental antigen
1010 challenge. *Mol Cell Proteomics* 4: 1251-1264.

1011 Yu, X.J., McGourty, K., Liu, M., Unsworth, K.E., and Holden, D.W. (2010) pH sensing by
1012 intracellular Salmonella induces effector translocation. *Science* 328: 1040-1043.

1013 Zimmerli, S., Edwards, S., and Ernst, J.D. (1996) Selective receptor blockade during phagocytosis
1014 does not alter the survival and growth of *Mycobacterium tuberculosis* in human macrophages. *Am J*
1015 *Respir Cell Mol Biol* 15: 760-770.

1016

1017

1018

FIGURE LEGENDS

FIGURE 1. Phagocytosis of *K. pneumoniae* by macrophages.

(A) Immunofluorescence confocal microscopy showing the lack of colocalisation between *K. pneumoniae* and the lysosome marker cathepsin D or TR-dextran (pulse-chase experiment described in Experimental procedures) in macrophages isolated from the BALF of infected mice with Kp43816R harbouring pFPV25.1Cm. Methanol fixation was used for cathepsin D staining. (B) Involvement of PI3K, cytoskeleton and lipid rafts on Kp43816R phagocytosis by MH-S cells. (C) Immunoblot analysis of Akt phosphorylation (P-Akt) in lysates of MH-S cells infected with live or UV-killed Kp43816R for the indicated times (in minutes). Membranes were probed for tubulin as a loading control. Images are representative of three independent experiments. (D) Immunoblot analysis of Akt phosphorylation (P-Akt) in lysates of PI3K inhibitor (LY294002) or DMSO (vehicle solution)-treated MH-S cells infected with Kp43816R for 20 min. Membranes were probed for tubulin as a loading control. Images are representative of three independent experiments.

FIGURE 2. Dynamics of *K. pneumoniae* survival in MH-S cells.

(A) MH-S cells were infected with Kp43816R for 30 min (MOI 50:1). Wells were washed and incubated with medium containing gentamicin (300 μg/ml) and polymyxin B (15 μg/ml) for 90 min to eliminate extracellular bacteria, and then with medium containing gentamicin 100 μg/ml for up to 7.5 h. Intracellular bacteria were quantified by lysis, serial dilution and viable counting on LB agar plates. (B) MH-S cells were infected with Kp43816R harboring pFPV25.1Cm and the percentage of macrophages containing intracellular bacteria (determined by extra-/intracellular differential staining**)** assessed over time. Extracellular bacteria were stained using rabbit anti-*Klebsiella* antibodies detected using donkey anti-rabbit conjugated to Rhodamine secondary antibodies. (C) Percentage of infected macrophages containing 1-2; 3-5, or more than 5 intracellular bacteria (determined by extra-/intracellular differential staining**)** over time. (D) MH-S cells were infected with Kp43816R harbouring pJT04mCherry, expressing mCherry constituvely, and pMMB207gfp3.1, expressing *gfpmut3.1* under the control of an IPTG-inducible promoter. IPTG (1

mM) was added 1.5 h before fixation. Images were taken 3.5 h post infection. Images are representative of duplicate coverslips in three independent experiments. (E) Percentage of intracellular bacteria (determined by extra-/intracellular differential staining; *Klebsiella* antibodies were detected using goat anti-rabbit conjugated to Cascade blue antibodies**)** mCherry-GFP positive over time. In panel A, data, shown as Log_{10}CFU/well, are the average of three independent experiments. In panel B, at least 500 cells belonging to three independent experiments were counted per time point whereas in panels C and E, at least 300 infected cells from three independent experiments were counted per time point.

FIGURE 3. Apoptosis of MH-S cells.

(A) MH-S cells were mock-treated or infected with Kp43816R harboring pFPV25.1Cm. 6 h post infection, cells were stained with Annexin V and 7-AAD and analysed by flow cytometry. A representative experiment of three is shown. (B) Data from three independent experiments are represented as mean ± SD.

FIGURE 4. Phagosome maturation during *K. pneumoniae* infection of MH-S cells.

(A) Upper and middle rows show the colocalization of Kp43816R harboring pFPV25.1Cm and EEA1 (images were taken 30 min post infection) and Lamp1 (images were taken 4 h post infection) using goat anti-EEA1 and donkey anti-goat conjugated to Rhodamine, and rat anti-Lamp-1 and donkey anti-rat conjugated to Rhodamine antibodies, respectively. Images are representative of triplicate coverslips in three independent experiments. (B) Panels show the colocalization of Kp431816R and Lamp1 and EGFP-Rab7 or RILP-C33-EGFP (images were taken 3.5 h post infection). Bacteria were stained using rabbit anti-*Klebsiella* and goat anti-rabbit conjugated to Cascade blue antibodies. Images are representative of triplicate coverslips in three independent experiments. (C) Percentage of Kp43816R colocalization with EEA1, Lamp1, and EGFP-Rab7 and RILP-C33-EGFP over a time course. Cells were infected, coverslips were fixed and stained at the indicated times. Values are given as mean percentage of Kp43816R colocalizing with the marker ±

SE. At least 300 infected cells belonging to three independent experiments were counted per time point.

FIGURE 5. Colocalization of *K. pneumoniae* with phagolysosomal markers.

(A) Upper row shows the colocalization of Kp43816R harboring pFPV25.1Cm and the dye LysoTracker at 4 h post infection. Middle row shows the colocalization of Kp43816R harboring pFPV25.1Cm and cathepsin D at 2 h post infection. Cathepsin D was stained using goat anti-human cathepsin D (G19) and donkey anti-goat conjugated to Rhodamine antibodies. Lower row displays the colocalization of Kp43816R harboring pFPV25.1Cm and TR-dextran at 2 h post infection. Images are representative of three independent experiments. (B) Percentage of Kp43816R colocalization with LysoTracker, cathepsin D and TR-dextran over a time course. Cells were infected, coverslips were fixed and stained at the indicated times. Values are given as mean percentage of Kp43816R colocalizing with the marker $\pm$ SE. At least 300 infected cells belonging to three independent experiments were counted per time point.

FIGURE 6. Effect of vacuolar acidification on *K. pneumoniae* survival.

(A) Microscopy analysis showing that bafilomycin A_1 (100 nM) treatment abrogates LysoTracker staining of the KCV (images were taken at 4 h post infection). MH-S cells were infected with Kp43816R harboring pFPV25.1Cm. Images are representative of triplicate coverslips in two independent experiments. (B) Experimental outline to investigate the effect of vacuolar acidification on the intracellular survival of Kp43816R. (C) Intracellular bacteria in MH-S cells, treated (white symbols) or not (black symbols) with bafilomycin A_1, were quantified by lysis, serial dilution and viable counting on LB agar plates. Data, shown as CFU/well, are the average of three independent experiments. Significance testing performed by Log Rank test. *, $P < 0.05$.

FIGURE 7. PI3K-AKT and Rab14 aid intracellular survival of *K. pneumoniae*.

(A) Quantification of intracellular bacteria in MH-S cells infected with Kp43816R which were mock-treated (black bar) or treated with LY294002 hydrochloride (75 μM) or with AKT X (10 μM). Treatments were added after the time of contact and kept until cells were lysed for bacterial

enumeration. Data, shown as CFU/well, are the average of three independent experiments. *, $P < 0.05$ (results are significantly different from the results for untreated cells; Mann-Whitney U test). (B) Percentage of Kp43816R colocalization with TR-dextran or cathepsin D in cells mock-treated or treated with the Akt inhibitor AKT X over a time course. Cells were infected, coverslips were fixed and stained at the indicated times. AKT X was added after the time of contact and kept until cells were fixed. Values are given as mean percentage of Kp43816R colocalizing with the marker $\pm$ SE. At least 300 infected cells belonging to three independent experiments were counted per time point. *, $P < 0.05$ (results are significantly different from the results for untreated cells; Mann-Whitney U test). (C) Colocalization of Kp431816R and Lamp1 and EGFP-Rab14 (images were taken 3.5 h post infection). Bacteria were stained using rabbit anti-*Klebsiella* and goat anti-rabbit conjugated to Cascade blue antibodies. Images are representative of triplicate coverslips in three independent experiments. (D) Percentage of Kp43816R colocalization with EGFP-Rab14 over a time course. Cells were infected, coverslips were fixed and stained at the indicated times. Values are given as mean percentage of Kp43816R colocalizing with the marker $\pm$ SE. At least 300 infected cells belonging to three independent experiments were counted per time point. (E) Quantification of intracellular bacteria in transfected MH-S cells with plasmid pcDNA3 or with Rab14 dominant-negative construct (DN-Rab14) at 3.5 h post infection. Data, shown as CFU/well, are the average of three independent experiments. *, $P < 0.05$ (results are significantly different from the results for cells transfected with control plasmid pcDNA3; Mann-Whitney U test). (F) Immunofluorescence showing the lack of colocalization of the KCV and EGFP-Rab14 (images were taken 3.5 h post infection) in AKT X treated cells. Bacteria were stained using rabbit anti-*Klebsiella* and goat anti-rabbit conjugated to Cascade blue antibodies. Images are representative of triplicate coverslips in two independent experiments.

FIGURE 8. Role of CPS in *K. pneumoniae* intracellular survival.

(A) MH-S or mTHP-1 cells were infected with Kp43816R (black symbols) or the capsule mutant (43Δ*manCKm*; white symbols). Intracellular bacteria were quantified by lysis, serial dilution and

viable counting on LB agar plates. Data, shown as Log_{10}CFU/well, are the average of three independent experiments. (B) Opsonization with 1% normal human sera (NHS) increased the phagocytosis of the capsule mutant (Kp43816Rdes) by mTHP-1 cells. Data, shown as CFU/well, are the average of three independent experiments. *, $P < 0.05$ (results are significantly different from the results for cells infected with the non-opsonized capsule mutant; Mann-Whitney U test); n.s., no significant difference. (C) mTHP-1 cells were infected for 30 min with Kp43816R or the capsule mutant (43Δ*manCKm*; Δ*manCKm*) which were either opsonized or not. Intracellular bacteria were quantified by lysis, serial dilution and viable counting on LB agar plates. Data, shown as Log_{10}CFU/well, are the average of three independent experiments. Significance testing performed by Log Rank test. *, $P < 0.05$. (D) Analysis of *cps::gfp* expression over time by flow cytometry. Analysis was performed staining the bacteria using rabbit anti-*Klebsiella* and donkey anti-rabbit conjugated to Rhodamine antibodies (red histogram). GFP fluorescence (green histogram) was analyzed in the gated Rhodamine labelled (antibody stained) population. Grey histogram represents GFP fluorescence for the negative-control sample, and the area of the histogram is considered negative for GFP fluorescence. Panels show the overlay of the different histograms. Results are representative of three independent experiments. (E) Fluorescence levels of Kp43816R containing pPROBE'43Procps. Data, shown as relative fluorescence units (RFUs), are the average of three independent experiments. *, $P < 0.05$ (results are significantly different from the results for cells grown in medium buffered to pH 7.5; Mann-Whitney U test). (F) *wzi*, *orf7* and *gnd* mRNA levels assessed by RT-qPCR. Data are presented as mean ± SD (n = 3).*, $P < 0.05$ (results are significantly different from the results for cells grown in medium buffered to pH 7.5; Mann-Whitney U test).

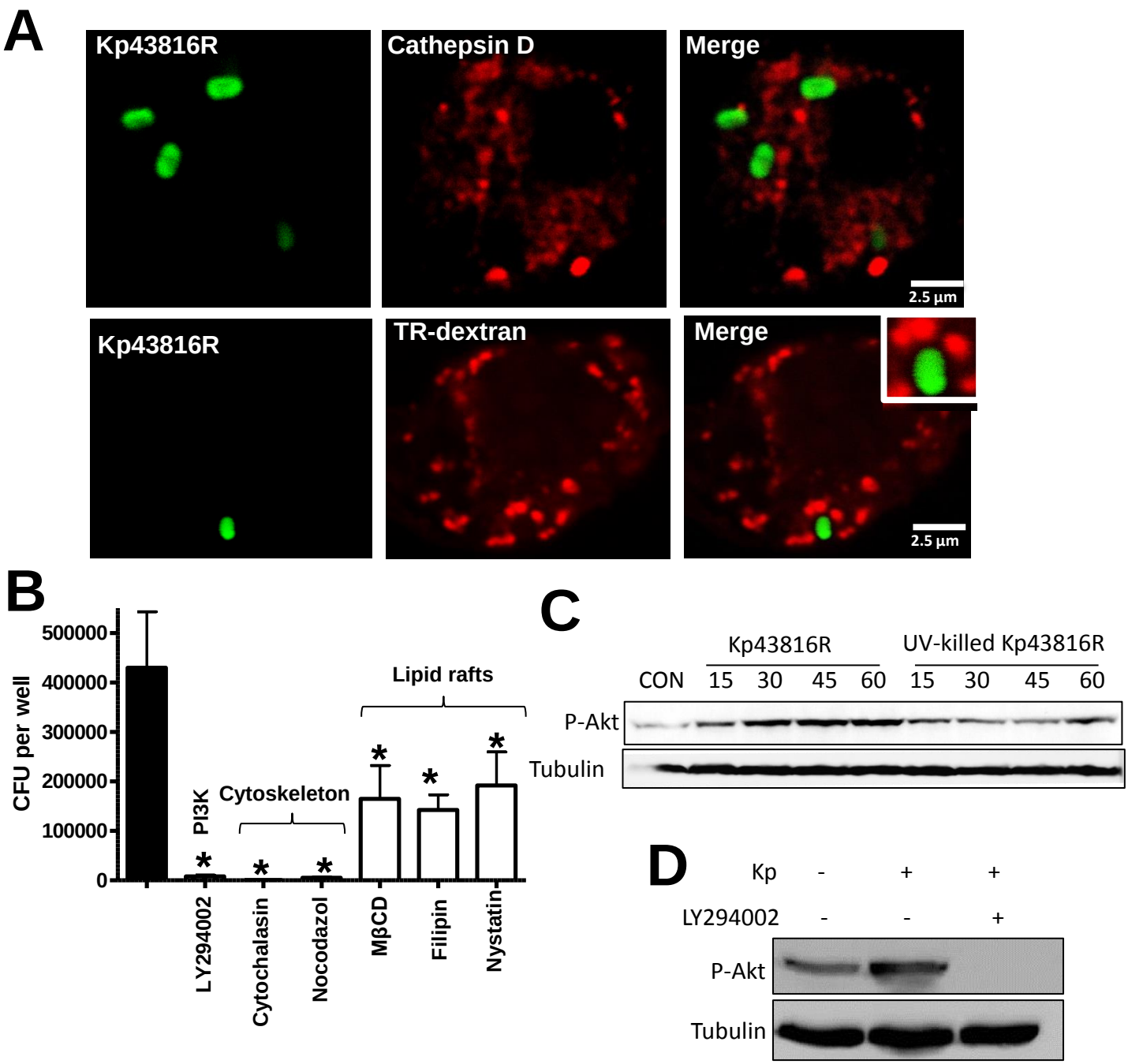
A
Kp43816R
Cathepsin D
Merge
2.5 µm
Kp43816R
TR-dextran
Merge
2.5 µm
B
CFU per well
500000
400000
300000
200000
100000
0
PI3K
Cytoskeleton
Lipid rafts
LY294002
Cytochalasin
Nocodazol
MβCD
Filipin
Nystatin
C
Kp43816R
UV-killed Kp43816R
CON
15
30
45
60
15
30
45
60
P-Akt
Tubulin
D
Kp
LY294002
P-Akt
Tubulin

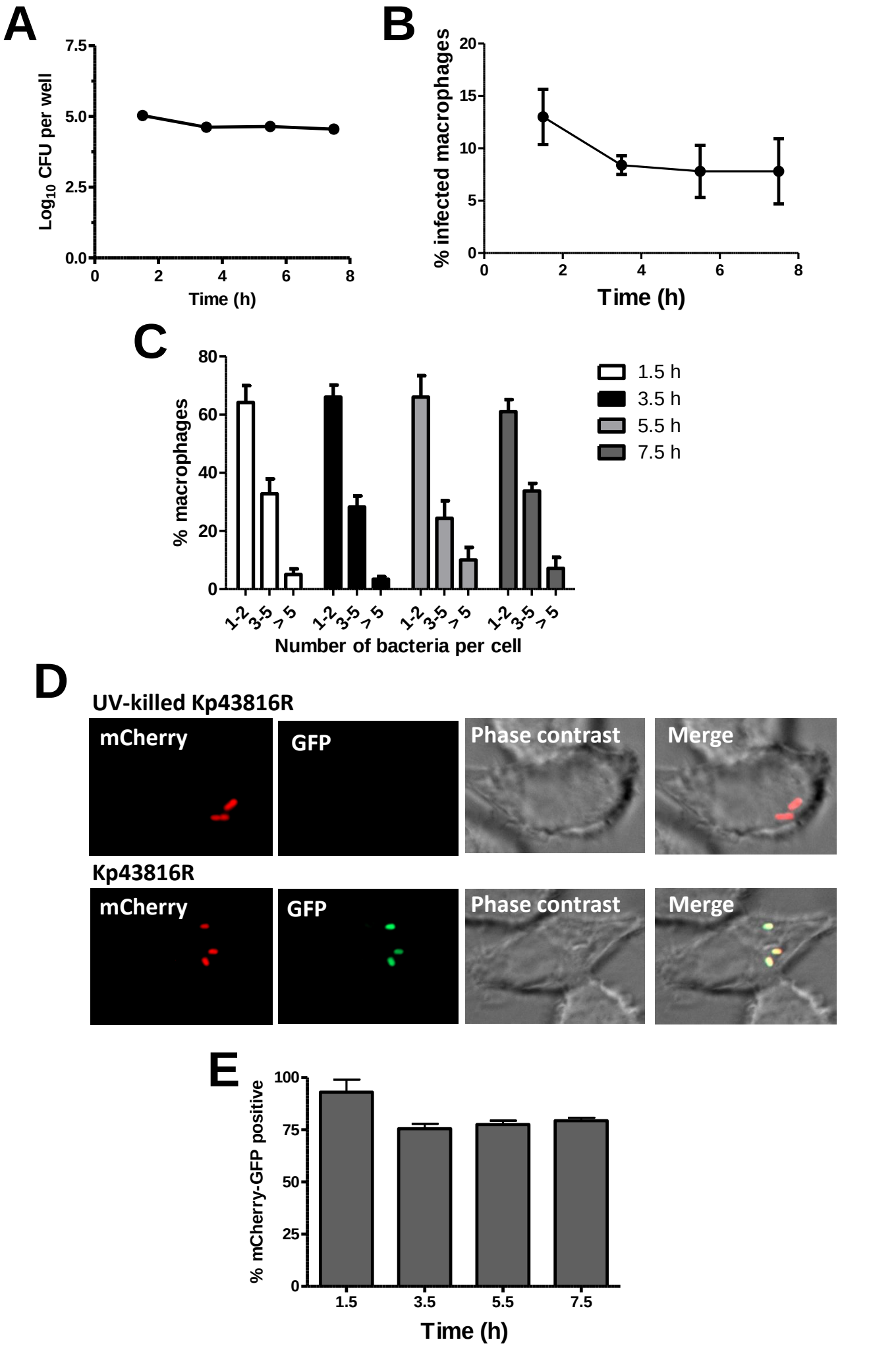
A
Log10 CFU per well
7.5
5.0
2.5
0.0
0
2
4
6
8
Time (h)
B
% infected macrophages
20
15
10
5
0
0
2
4
6
8
Time (h)
C
% macrophages
80
60
40
20
0
1-2
3-5
>5
1.5 h
3.5 h
5.5 h
7.5 h
Number of bacteria per cell
D
UV-killed Kp43816R
mCherry
GFP
Phase contrast
Merge
Kp43816R
mCherry
GFP
Phase contrast
Merge
E
% mCherry-GFP positive
100
75
50
25
0
1.5
3.5
5.5
7.5
Time (h)

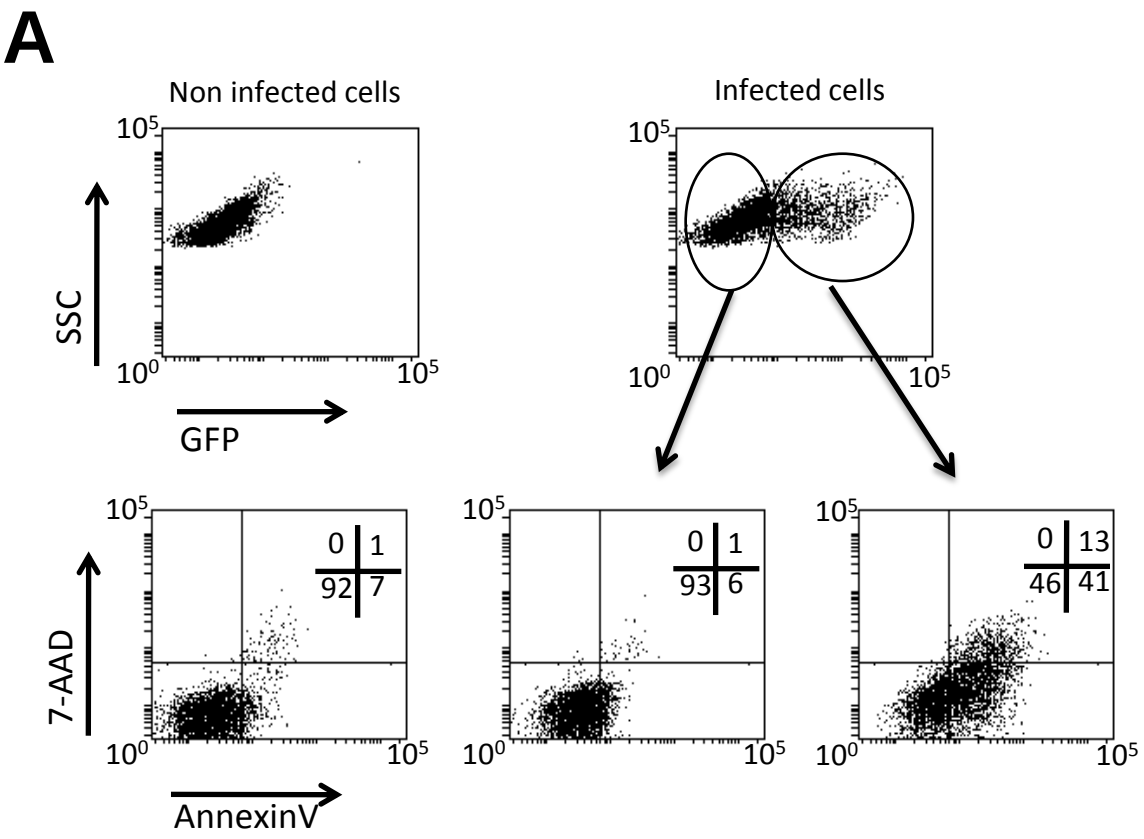
A
Non infected cells
Infected cells
SSC
GFP
7-AAD
AnnexinV
0
1
92
7
0
1
93
6
0
13
46
41

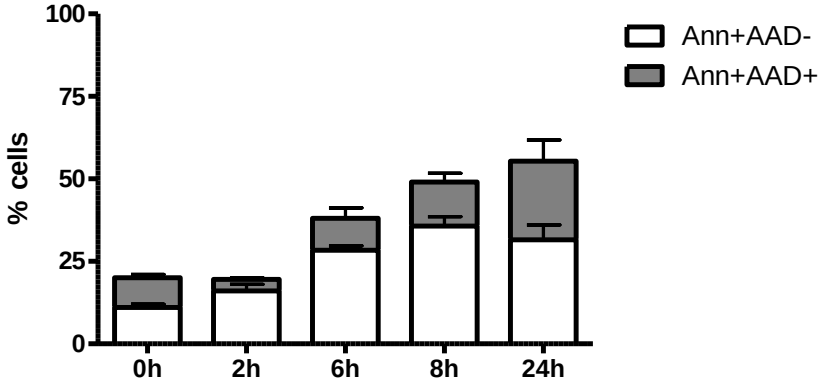
B
% cells
Ann+AAD-
Ann+AAD+
0h
2h
6h
8h
24h

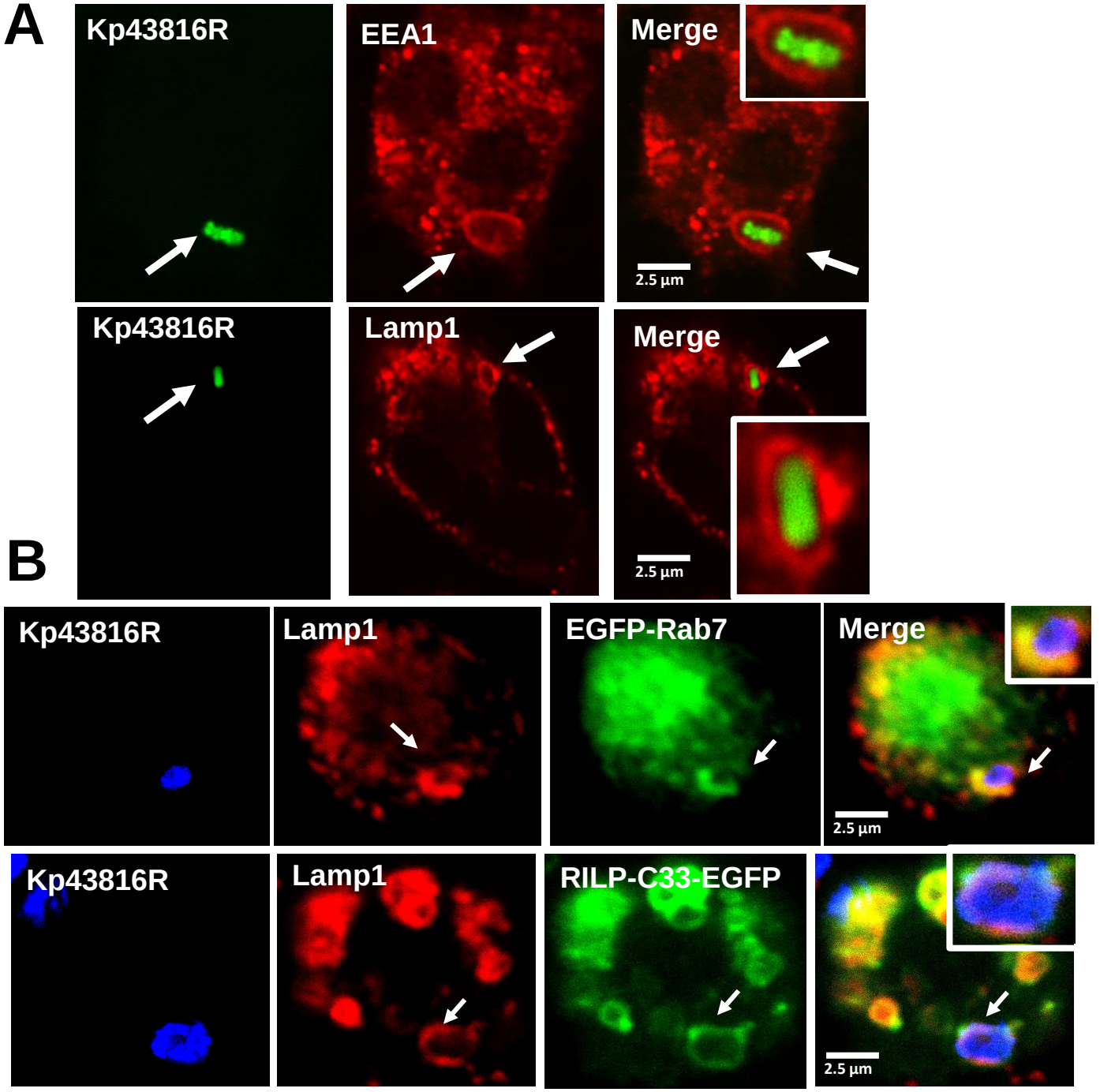
A
Kp43816R
EEA1
Merge
2.5 µm
Kp43816R
Lamp1
Merge
2.5 µm
B
Kp43816R
Lamp1
EGFP-Rab7
Merge
2.5 µm
Kp43816R
Lamp1
RILP-C33-EGFP
2.5 µm

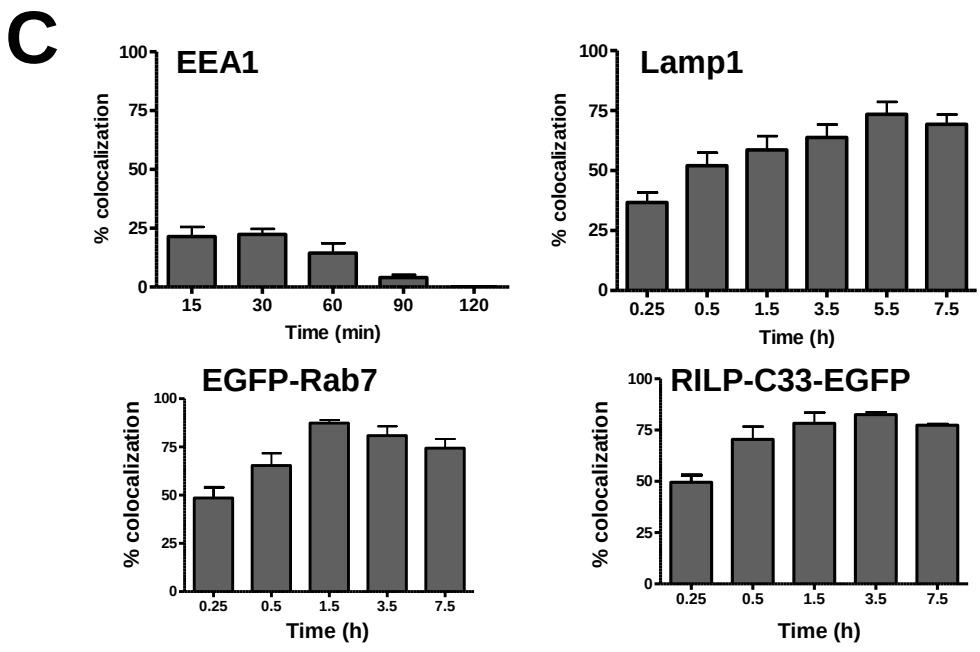
C
EEA1
% colocalization
100
75
50
25
0
15
30
60
90
120
Time (min)
Lamp1
% colocalization
100
75
50
25
0
0.25
0.5
1.5
3.5
5.5
7.5
Time (h)
EGFP-Rab7
% colocalization
100
75
50
25
0
0.25
0.5
1.5
3.5
7.5
Time (h)
RILP-C33-EGFP
% colocalization
100
75
50
25
0
0.25
0.5
1.5
3.5
7.5
Time (h)

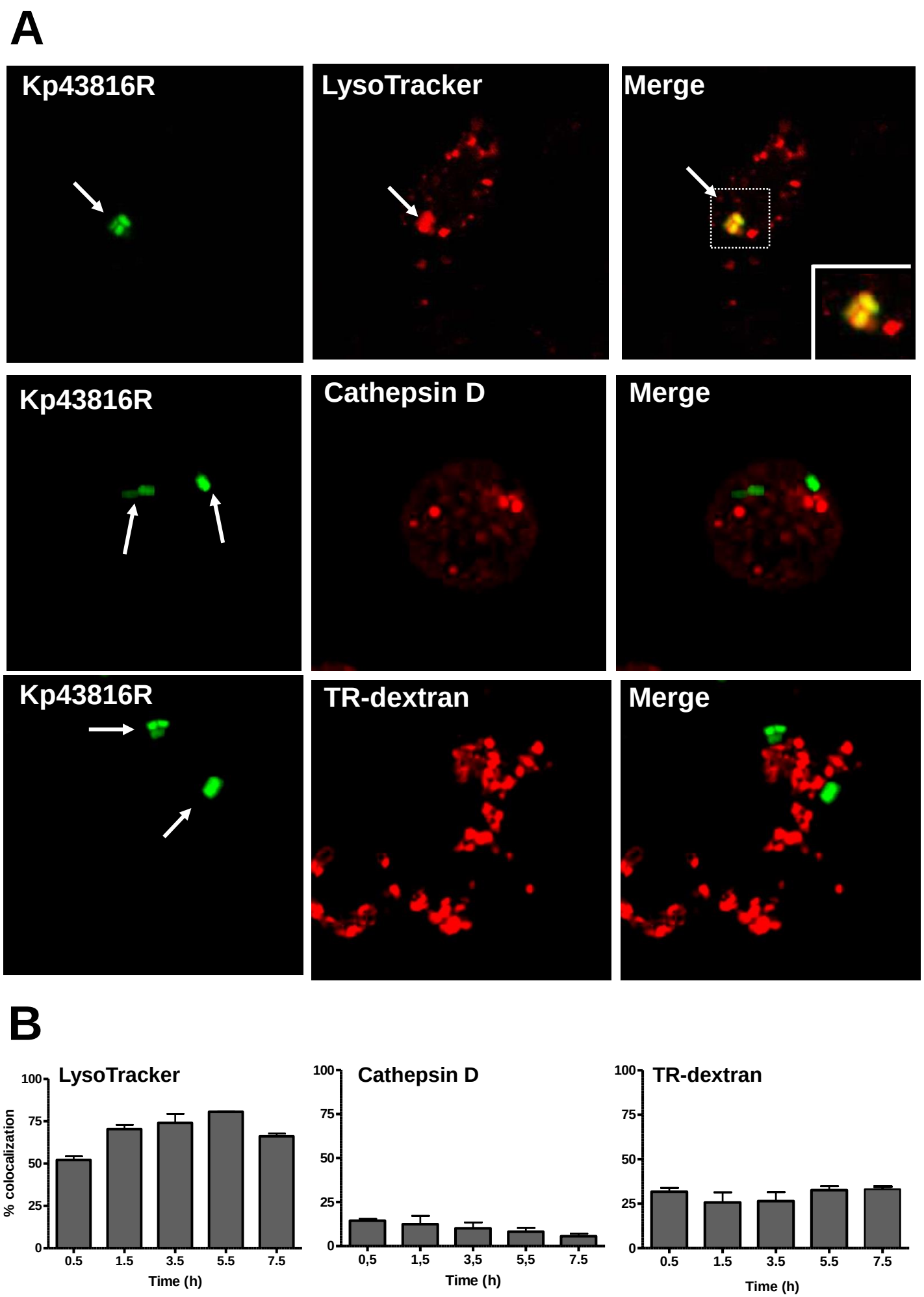
A
Kp43816R
LysoTracker
Merge
Kp43816R
Cathepsin D
Merge
Kp43816R
TR-dextran
Merge
B
LysoTracker
% colocalization
100
75
50
25
0
0.5
1.5
3.5
5.5
7.5
Time (h)
Cathepsin D
100
75
50
25
0
0,5
1,5
3,5
5,5
7.5
Time (h)
TR-dextran
100
75
50
25
0
0.5
1.5
3.5
5.5
7.5
Time (h)

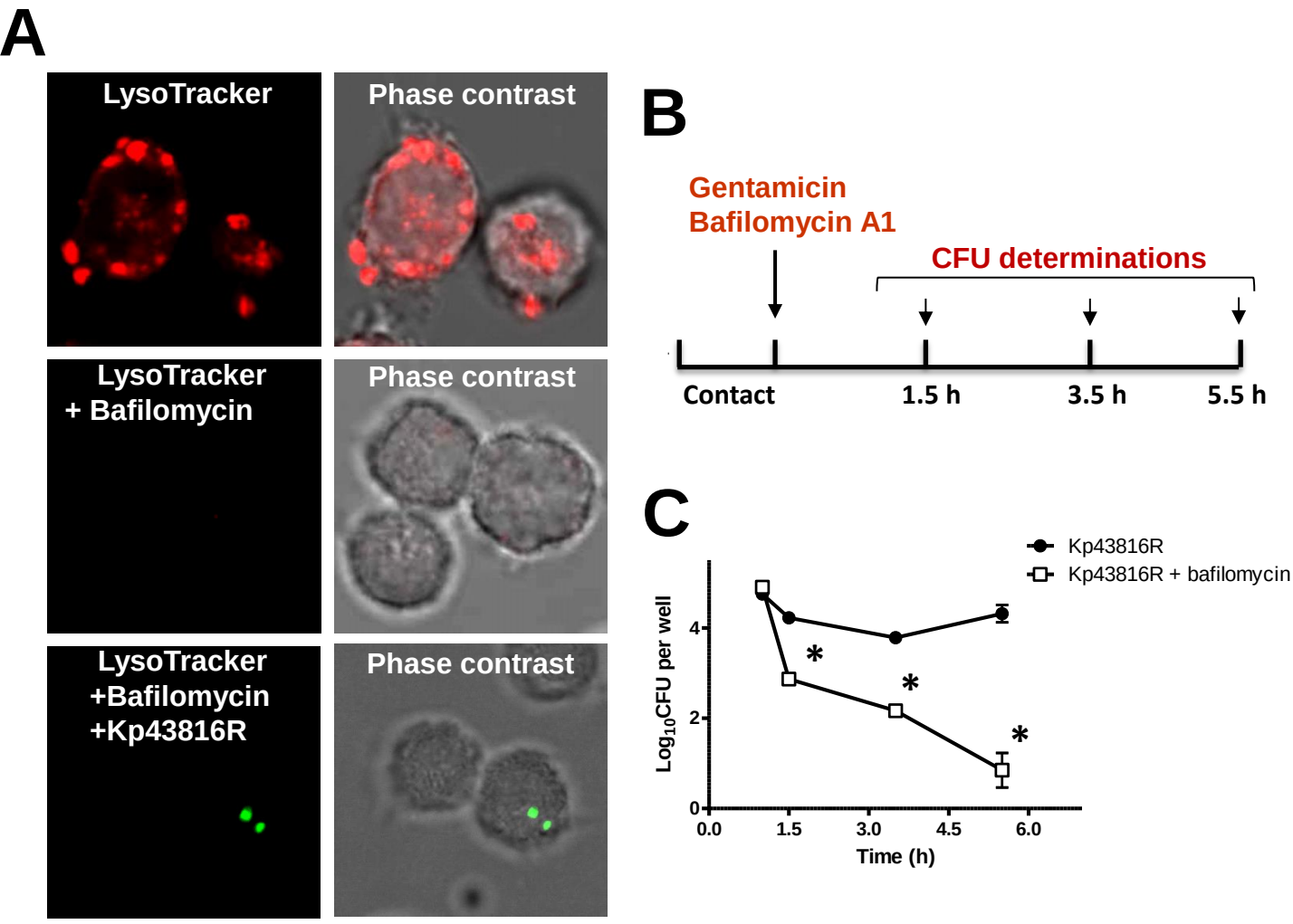
A
LysoTracker
Phase contrast
LysoTracker
+ Bafilomycin
Phase contrast
LysoTracker
+Bafilomycin
+Kp43816R
Phase contrast
B
Gentamicin
Bafilomycin A1
CFU determinations
Contact
1.5 h
3.5 h
5.5 h
C
Kp43816R
Kp43816R + bafilomycin
Log10CFU per well
0
2
4
0.0
1.5
3.0
4.5
6.0
Time (h)
*
*
*

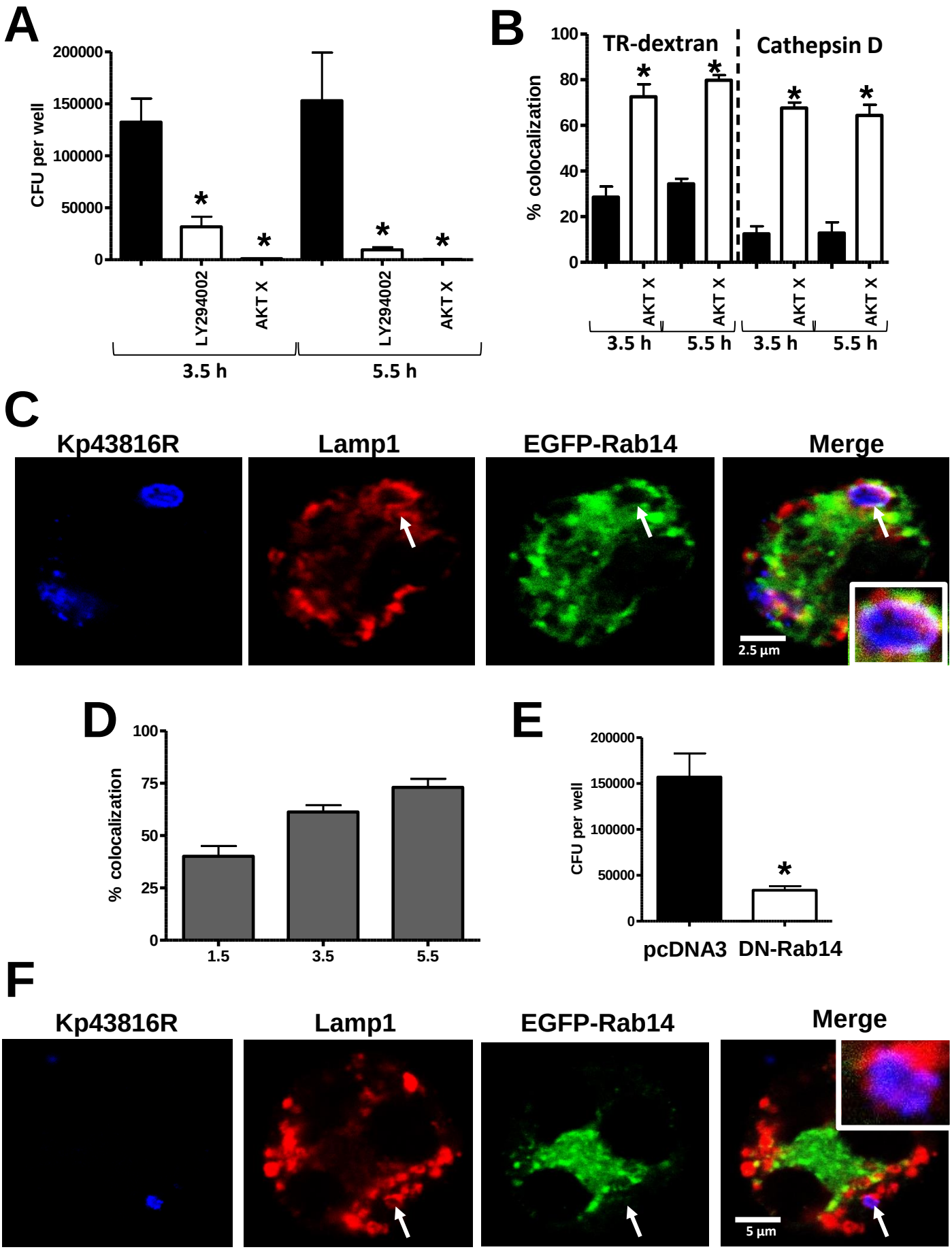
A
CFU per well
200000
150000
100000
50000
0
LY294002
AKT X
LY294002
AKT X
3.5 h
5.5 h
B
% colocalization
100
80
60
40
20
0
TR-dextran
Cathepsin D
AKT X
AKT X
AKT X
AKT X
3.5 h
5.5 h
3.5 h
5.5 h
C
Kp43816R
Lamp1
EGFP-Rab14
Merge
2.5 µm
D
% colocalization
100
75
50
25
0
1.5
3.5
5.5
E
CFU per well
200000
150000
100000
50000
0
pcDNA3
DN-Rab14
F
Kp43816R
Lamp1
EGFP-Rab14
Merge
5 µm

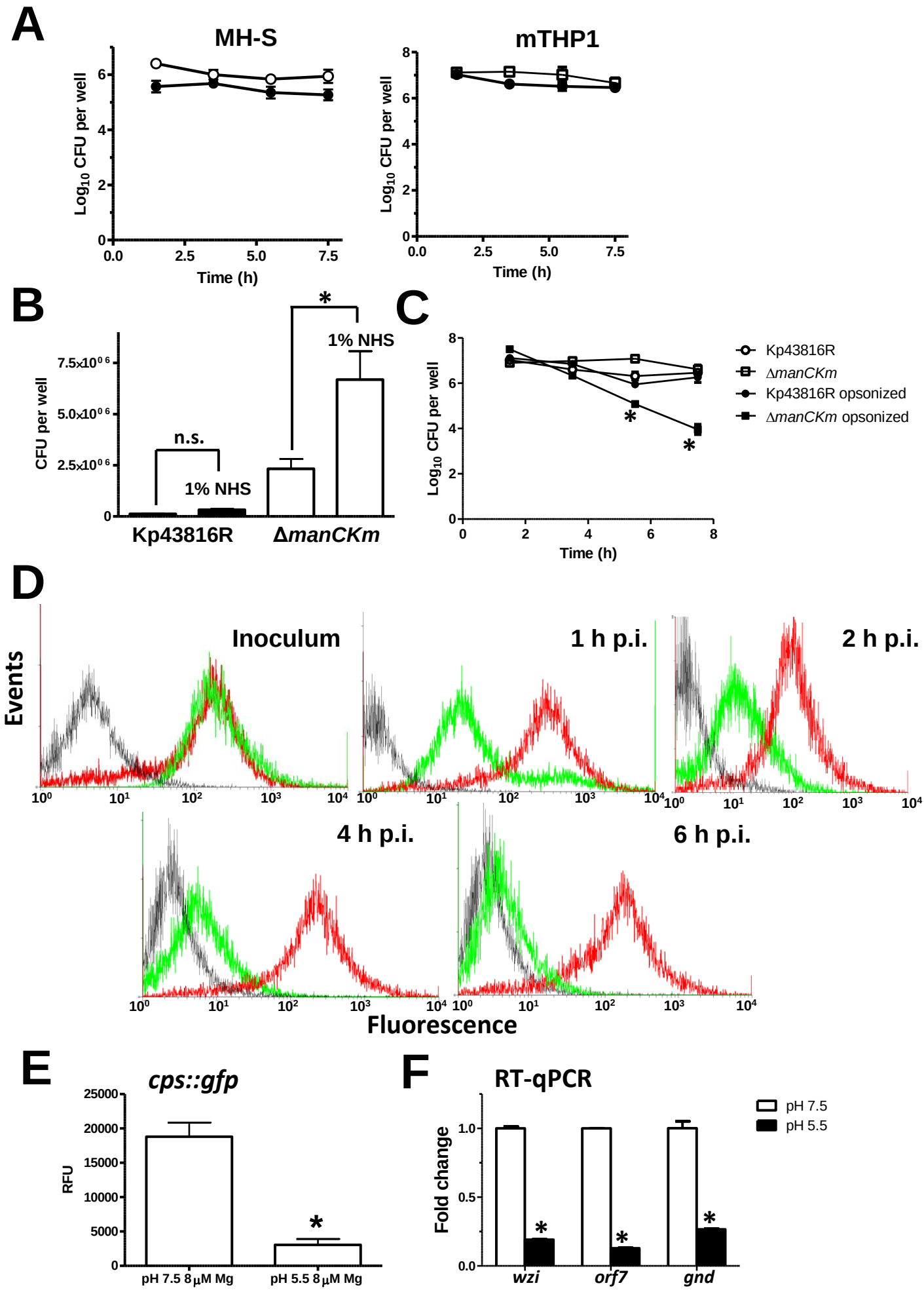
A
MH-S
mTHP1
Log10 CFU per well
Time (h)
B
1% NHS
n.s.
CFU per well
Kp43816R
ΔmanCKm
C
Kp43816R
ΔmanCKm
Kp43816R opsonized
ΔmanCKm opsonized
D
Inoculum
1 h p.i.
2 h p.i.
4 h p.i.
6 h p.i.
Events
Fluorescence
E
cps::gfp
RFU
pH 7.5 8 μM Mg
pH 5.5 8 μM Mg
F
RT-qPCR
pH 7.5
pH 5.5
Fold change
wzi
orf7
gnd